

# Trivalent Lanthanide Selenolates and Tellurolates Incorporating Sterically Hindered Ligands and Their Characterization by Multinuclear NMR Spectroscopy and X-ray Crystallography

Douglas R. Cary, Graham E. Ball, and John Arnold\*

Contribution from the Department of Chemistry, University of California, Berkeley, California 94720

Received November 7, 1994<sup>§</sup>

**Abstract:** Homoleptic trivalent selenolates of La and Y have been isolated from the reaction of  $\text{Ln}[\text{N}(\text{SiMe}_3)_2]_3$  ( $\text{Ln} = \text{La}, \text{Ce}$ ) with  $3\text{HSeSi}(\text{SiMe}_3)_3$  in hexanes. Variable-temperature NMR studies suggest that  $\text{La}[\text{SeSi}(\text{SiMe}_3)_3]_3$  behaves as a three-coordinate monomer in toluene, whereas data for the Y analogue are consistent with the dimeric structure  $\{\text{Y}[\text{SeSi}(\text{SiMe}_3)_3]_2[\mu\text{-SeSi}(\text{SiMe}_3)_3]_2\}$ . EXSY experiments have been used to investigate ligand exchange in the Y compound. THF adducts  $\text{Ln}[\text{TeSi}(\text{SiMe}_3)_3]_3(\text{THF})_2$  ( $\text{Ln} = \text{La}, \text{Sm}, \text{Yb}$ ) have been isolated and fully characterized. Tellurolate species  $\text{Ln}[\text{TeSi}(\text{SiMe}_3)_3]_3$  ( $\text{Ln} = \text{La}, \text{Ce}$ ), prepared by the analogous reaction with  $3\text{HTeSi}(\text{SiMe}_3)_3$  in hydrocarbons, were characterized by NMR spectroscopy and by the isolation of derivatives. Addition of DMPE (DMPE = 1,2-bis(dimethylphosphino)ethane) to these reactions gave isolable adducts  $\text{Ln}[\text{TeSi}(\text{SiMe}_3)_3]_3(\text{DMPE})_2$  ( $\text{Ln} = \text{La}, \text{Ce}, \text{Y}$ ) which have been characterized by multinuclear and variable-temperature NMR spectroscopy. In addition, the X-ray crystal structure of  $\text{La}[\text{TeSi}(\text{SiMe}_3)_3]_3(\text{DMPE})_2$  has been determined: it crystallizes at  $-40^\circ\text{C}$  from hexanes in the space group  $C2/c$  with  $a = 51.207(11)\text{ \AA}$ ,  $b = 15.725(3)\text{ \AA}$ ,  $c = 18.903(3)\text{ \AA}$ ,  $\beta = 92.698(15)^\circ$ ,  $V = 15204(9)\text{ \AA}^3$ ,  $d_{\text{calcd}} = 1.37\text{ g cm}^{-3}$ , and  $Z = 8$ . Exchange spectroscopy has also been used to investigate the process by which these molecules rearrange in solution. The homoleptic tellurolates are unstable in solution as monitored by NMR spectroscopy; preparative-scale reactions led to the isolation of a remarkable tellurolate/telluride cluster  $\text{Ce}_5\text{Te}_3[\text{TeSi}(\text{SiMe}_3)_3]_9$ , which has been structurally characterized by X-ray crystallography.  $\text{Ce}_5\text{Te}_3[\text{TeSi}(\text{SiMe}_3)_3]_9$  crystallizes at  $-40^\circ\text{C}$  from hexanes in the space group  $P6_3/m$  with  $a = 20.456(5)\text{ \AA}$ ,  $b = 20.456(5)\text{ \AA}$ ,  $c = 28.063(9)\text{ \AA}$ ,  $\gamma = 120^\circ$ ,  $V = 10170(8)\text{ \AA}^3$ ,  $d_{\text{calcd}} = 1.46\text{ g cm}^{-3}$ , and  $Z = 2$ .

## Introduction

The ability of sterically hindered ligands to stabilize low-molecularity metal chalcogenolates is now well-documented.<sup>1–4</sup> Even for the heavier chalcogens, which have a pronounced tendency to bridge metal centers,<sup>5–7</sup> monomeric and dimeric species can be prepared. Research in our group has shown that the  $-\text{ESi}(\text{SiMe}_3)_3$  ( $\text{E} = \text{S}, \text{Se}, \text{Te}$ ) ligands<sup>8</sup> are useful in the formation of well-defined, easily-prepared species with a range of metals and non-metals throughout the periodic table.<sup>3,5,9–16</sup> Recently, we extended these studies to include trivalent and

divalent lanthanide chalcogenolates.<sup>3,17</sup> Interest in compounds of this type has grown recently<sup>4,18–20</sup> with the realization that they may be used as precursors to semiconducting lanthanide chalcogenides  $\text{LnE}$  ( $\text{Ln} = \text{Sm}, \text{Eu}, \text{Yb}$ ).<sup>21</sup>

As part of a comprehensive exploration of lanthanide and

<sup>§</sup> Abstract published in *Advance ACS Abstracts*, March 1, 1995.

(1) For reviews of alkoxide and thiolate chemistry, see: Bradley, D. C.; Mehrotra, R. C.; Gaur, D. P. *Metal Alkoxides*; Academic: New York, 1978. Mehrotra, R. C.; Singh, A.; Tripathi, U. M. *Chem. Rev.* **1991**, *91*, 1287. Blower, P. J.; Dilworth, J. R. *Coord. Chem. Rev.* **1987**, *76*, 121.

(2) See the following and references within: Bochmann, M.; Bwembya, G. C.; Grinter, R.; Powell, A. K.; Webb, K. J.; Hursthouse, M. B.; Malik, K. M. A.; Mazid, M. A. *Inorg. Chem.* **1994**, *33*, 2290. Ruhlandt-Senge, K.; Power, P. P. *Inorg. Chem.* **1993**, *32*, 4505. Gladyshev, E. N.; Vyazankin, N. S.; Andreevichev, V. S.; Klumov, A. A.; Razuvaev, G. A. *J. Organomet. Chem.* **1971**, *28*, C42.

(3) Cary, D. R.; Arnold, J. *Inorg. Chem.* **1994**, *33*, 1791.

(4) Strzelecki, A. R.; Tlinski, P. A.; Hessel, B. A.; Bianconi, P. A. *J. Am. Chem. Soc.* **1992**, *114*, 3159.

(5) Arnold, J. *Prog. Inorg. Chem.*, in press.

(6) Gysling, H. J. In *The Chemistry of Organic Selenium and Tellurium Compounds*; Patai, S.; Rappoport, Z., Eds.; Wiley: New York, 1986; Vol. 1, Chapter 18.

(7) Dance, I. G. *Polyhedron* **1986**, *5*, 1037.

(8) Bonasia, P. J.; Christou, V.; Arnold, J. *J. Am. Chem. Soc.* **1993**, *115*, 6777.

(9) Bonasia, P. J.; Arnold, J. *Inorg. Chem.* **1992**, *31*, 2508.

(10) Bonasia, P. J.; Mitchell, G. P.; Hollander, F. J.; Arnold, J. *Inorg. Chem.* **1994**, *33*, 1797.

(11) Christou, V.; Arnold, J. *J. Am. Chem. Soc.* **1992**, *114*, 6240.

(12) Christou, V.; Arnold, J. *Angew. Chem., Int. Ed. Engl.* **1993**, *32*, 1450.

(13) Christou, V.; Wuller, S. P.; Arnold, J. *J. Am. Chem. Soc.* **1993**, *115*, 10545.

(14) Gindelberger, D. E.; Arnold, J. *Inorg. Chem.* **1994**, *33*, 6293.

(15) Gindelberger, D. E.; Arnold, J. *Inorg. Chem.* **1993**, *32*, 5813.

(16) Sellgson, A. L.; Arnold, J. *J. Am. Chem. Soc.* **1993**, *115*, 8214.

(17) Cary, D. R.; Arnold, J. *J. Am. Chem. Soc.* **1993**, *115*, 2520.

(18) Cetinkaya, B.; Hitchcock, P. B.; Lappert, M. F.; Smith, R. G. *J. Chem. Soc., Chem. Commun.* **1992**, 932.

(19) See the following and references within: Brewer, M.; Khasnis, D. V.; Buretea, M.; Berardini, M.; Emge, T. J.; Brennan, J. G. *Inorg. Chem.* **1994**, *33*, 2743. Berardini, M.; Emge, T.; Brennan, J. G. *J. Am. Chem. Soc.* **1994**, *116*, 6941. Khasnis, D. V.; Brewer, M.; Lee, J.; Emge, T. J.; Brennan, J. G. *J. Am. Chem. Soc.* **1994**, *116*, 7129. Mashima, K.; Nakayama, Y.; Nakamura, A.; Kanehisa, N.; Kai, Y.; Takaya, H. *J. Organomet. Chem.* **1994**, *473*, 85. Edelmann, F. T.; Rieckhoff, M.; Haiduc, I.; Silaghi-Dumitrescu, I. *J. Organomet. Chem.* **1993**, *447*, 203. Tatsumi, K.; Amemlya, T.; Kawaguchi, H.; Tani, K. *J. Chem. Soc., Chem. Commun.* **1993**, 773. Berg, D. J.; Andersen, R. A.; Zalkin, A. *Organometallics* **1988**, *7*, 1858. Rad'kov, Y. F.; Fedorova, E. A.; Khorshev, S. Y.; Kallina, G. S.; Bochkarev, M. N.; Razuvaev, G. A. *Russ. J. Gen. Chem. (Engl. Trans.)* **1985**, *55*, 1911. Aspnall, H. C.; Bradley, D. C.; Hursthouse, M. B.; Sales, K. D.; Walker, N. P. C. *J. Chem. Soc., Chem. Commun.* **1985**, 1585. For examples of related lanthanide chalcogenide complexes, see: Evans, W. J.; Rabe, G. W.; Ziller, J. W.; Doedens, R. J. *Inorg. Chem.* **1994**, *33*, 2719. Berg, D. J.; Burns, C. J.; Andersen, R. A.; Zalkin, A. *Organometallics* **1989**, *8*, 1865.

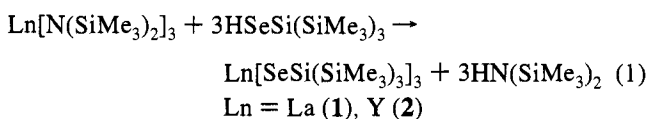
(20) See the following and references within: Piers, W. E.; Ferguson, G.; Gallagher, J. F. *Inorg. Chem.* **1994**, *33*, 3784. Beletskaya, I. P.; Voskoboinikov, A. Z.; Shestakova, A. K.; Yanovsky, A. I.; Fukin, G. K.; Zacharov, L. N.; Struchkov, Y. T.; Schumann, H. *J. Organomet. Chem.* **1994**, *468*, 121. Kapur, S.; Kalsotra, B. L.; Multani, R. K. *J. Inorg. Nucl. Chem.* **1973**, *35*, 3966.

(21) *Handbook of the Physics and Chemistry of Rare Earths*; Gschneidner, K. A., Eyring, L., Eds.; North-Holland: Amsterdam, 1978.

group 3 chalcogenolates, we have examined the chemistry of the trivalent complexes, since the +3 oxidation state is by far the most prevalent for these metals. It is widely accepted that bonding in complexes of the lanthanide metals is primarily ionic, with the size of the metal determining reactivity.<sup>22</sup> In our studies, we chose to prepare complexes of some of the largest (La, Ce) and the smallest (Yb, Y, Sc) members of the series, in order to compare the effects of size on the structures and chemistry of the compounds. In addition, we have investigated trivalent Sm, Eu, and Yb chalcogenolates in order to examine the reactivity of complexes with easily-reduced metal centers. Some aspects of this work have been communicated.<sup>17</sup>

## Results and Discussion

**Selenolate Derivatives.** The protonolysis reaction between  $\text{Ln}[\text{N}(\text{SiMe}_3)_2]_3$  ( $\text{Ln} = \text{La}, \text{Y}$ ) and  $\text{HSeSi}(\text{SiMe}_3)_3$  in hydrocarbon solvents provides a simple method of preparing trivalent lanthanide selenolates (eq 1).



Monitoring of these reactions by  $^1\text{H}$  NMR spectroscopy indicated quantitative conversion to products. On preparative scales, crystallization from hexanes affords pale yellow powders of analytically pure **1** and **2** in yields that typically range from 40 to 60%. The high solubility of these compounds in most noncoordinating organic solvents is primarily responsible for the moderate yields. Compounds **1** and **2** are both air- and moisture-sensitive, but under dry nitrogen they are stable in the solid state for several days at room temperature under ambient lighting. Under similar conditions in benzene- $d_6$ , **1** and **2** show about 30% and 5% decomposition, respectively, by NMR spectroscopy after 24 h. Both compounds, as well as all of the isolated complexes described below, can be stored for at least 2 weeks in the solid state at  $-40^\circ\text{C}$  without any noticeable change in sample purity.

Variable-temperature and multinuclear NMR studies have been valuable in determining the solution-state properties of these molecules. The  $^1\text{H}$ ,  $^{13}\text{C}\{^1\text{H}\}$ , and  $^{77}\text{Se}\{^1\text{H}\}$  NMR spectra of **1** show singlets for the equivalent selenolate ligands at 0.46, 1.52, and 537 ppm, respectively. The  $^{77}\text{Se}$  nuclei are significantly deshielded, in common with related complexes of this ligand with electropositive metals.<sup>8</sup> These signals do not broaden or shift significantly from 24 to  $-80^\circ\text{C}$  which, together with its high solubility in nonpolar solvents, suggests that **1** behaves as a rare example<sup>18,23–27</sup> of a three-coordinate monomeric lanthanide complex in solution. Unfortunately, slow decomposition in solution prevented accurate molecular weight determinations to further support this conclusion.

In contrast, the solution behavior of **2** is consistent with the formation of a dimeric complex. At room temperature, the  $^1\text{H}$  NMR spectrum shows two slightly broadened singlets in the ratio 1:2 at 0.58 and 0.40 ppm. The  $^{13}\text{C}\{^1\text{H}\}$  spectrum also

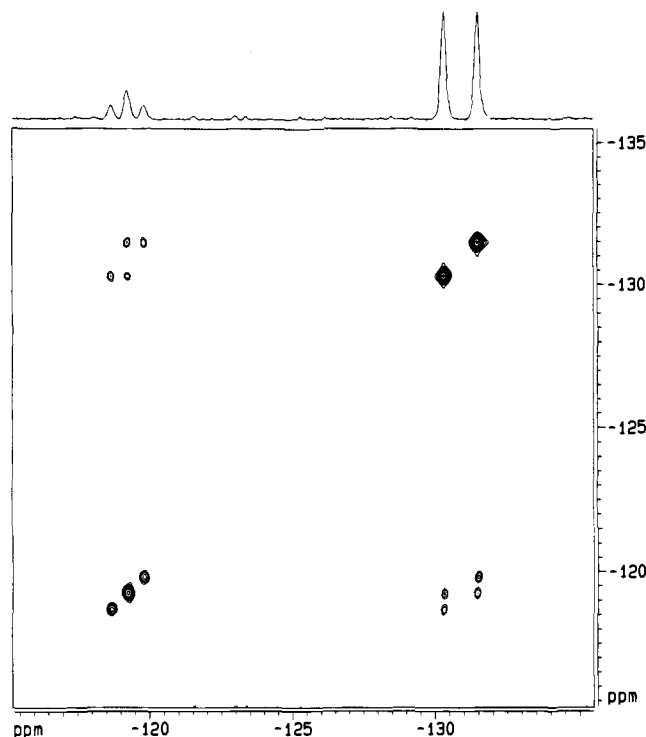


**Figure 1.**  $^{77}\text{Se}\{^1\text{H}\}$  EXSY spectrum of  $\{\text{Y}[\text{SeSi}(\text{SiMe}_3)_3]_2[\mu\text{-SeSi}(\text{SiMe}_3)_3]_2\}$  (**2**) at  $25^\circ\text{C}$  (20 ms mixing time). The vertical projection shows the normal 1D spectrum.

shows two inequivalent ligand resonances at 2.60 and 1.38 ppm in the same ratio. Cooling the sample to  $0^\circ\text{C}$  sharpens the signals in both spectra. In the  $^{77}\text{Se}\{^1\text{H}\}$  NMR spectra ( $^{77}\text{Se}$ ,  $I = 1/2$ , 7.6%) at 22 and  $0^\circ\text{C}$ , a 1:2 ratio is again seen between the two signals, but coupling to  $^{89}\text{Y}$  ( $I = 1/2$ , 100% abundance) gives rise to a more informative spectrum (see top of Figure 1). The triplet at  $-122$  ppm ( $|^1J_{\text{Y-Se}}| = 32.1$  Hz) and the doublet at  $-130$  ppm ( $|^1J_{\text{Y-Se}}| = 65.1$  Hz) in the ratio 1:2 are assigned to the two bridging and four terminal selenolate ligands, respectively, of the dimer. The slightly broadened peaks observed at ambient temperatures indicate slow exchange between bridging and terminal ligands on the NMR time scale. In order to probe the mechanism of this exchange, the  $^{77}\text{Se}\{^1\text{H}\}$  EXSY spectrum was obtained (Figure 1). The lack of cross peaks surrounding the downfield triplet indicates that the lowest energy ligand exchange process does not involve dissociation of the dimer into monomers.

Confirmation of the Se–Y couplings is supplied by the low-temperature  $^{89}\text{Y}$  NMR spectrum, which shows an extremely low-field singlet at 995 ppm with two sets of  $^{77}\text{Se}$  satellites in the appropriate positions (Figure 2). Upon heating a sample of **2** in toluene- $d_8$ , ligand exchange is more rapid with coalescence of the two signals occurring at about  $65^\circ\text{C}$  in the  $^1\text{H}$  NMR spectrum. At  $100^\circ\text{C}$ , both the  $^1\text{H}$  and  $^{13}\text{C}\{^1\text{H}\}$  NMR spectra show a single broad resonance, indicating that ligand exchange is still fast at this temperature (no  $^{77}\text{Se}\{^1\text{H}\}$  NMR signals were detected). The situation is complicated by partial decomposition of the sample at this temperature ( $<5\%$ ) which effectively ruled out further measurements. Bridging ligands are quite common in low-coordinate complexes of the smaller lanthanide elements;<sup>28</sup> the disparity in the structures of **1** and **2** in solution may simply be a result of the differing metal radii ( $r = 1.17$  and  $1.04$  Å, respectively).<sup>29</sup>

(28) Schumann, H. *Angew. Chem., Int. Ed. Engl.* **1984**, *23*, 474.

(29) Shannon, R. D. *Acta Crystallogr., Sect. A* **1976**, *A32*, 751. Unless stated otherwise, all values given are the crystal radii for coordination number 6.

(22) Cotton, F. A.; Wilkinson, G. *Advanced Inorganic Chemistry*, 5th ed.; Wiley: New York, 1988; Chapter 20.

(23) Herrmann, W. A.; Anwander, R.; Scherer, W. *Chem. Ber.* **1993**, *126*, 1533.

(24) Hitchcock, P. B.; Lappert, M. F.; Smith, R. G.; Bartlett, R. A.; Power, P. P. *J. Chem. Soc., Chem. Commun.* **1988**, 1007.

(25) Hitchcock, P. B.; Lappert, M. F.; Singh, A. *J. Chem. Soc., Chem. Commun.* **1983**, 1499.

(26) Bradley, D. C.; Ghotra, J. S.; Hart, F. A. *Inorg. Nucl. Chem. Lett.* **1976**, *12*, 735.

(27) Bradley, D. C.; Ghotra, J. S.; Hart, F. A. *J. Chem. Soc., Dalton Trans* **1973**, 1021.

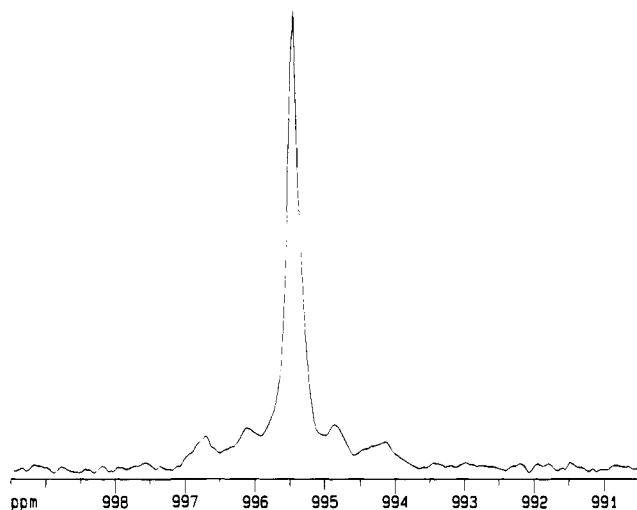
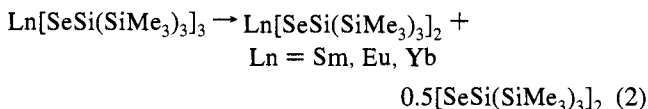


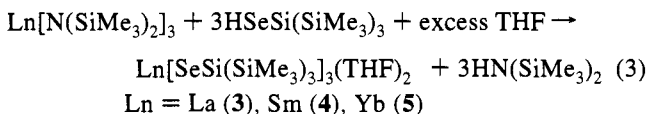
**Figure 2.**  $^{89}\text{Y}$  NMR spectrum of  $\{\text{Y}[\text{SeSi}(\text{SiMe}_3)_3]_2[\mu\text{-SeSi}(\text{SiMe}_3)_3]\}_2$  (**2**) at 0 °C.

Size effects clearly play a role in attempts to prepare homoleptic Sc ( $\text{Sc}^{3+}$ ,  $r = 0.89 \text{ \AA}$ )<sup>29</sup> selenolates. Thus, no reaction is observed between  $\text{Sc}[\text{N}(\text{SiMe}_3)_2]_3$  and  $\text{HSeSi}(\text{SiMe}_3)_3$  over 6 h at room temperature in benzene- $d_6$  and heating to 100 °C for 16 h results in consumption of only about half of the starting materials and the formation of a complicated mixture of products. Similar problems have been noted in the preparation of sterically hindered lanthanide alkoxides.<sup>23</sup>

Reactions of  $\text{Ln}[\text{N}(\text{SiMe}_3)_2]_3$  ( $\text{Ln} = \text{Sm}, \text{Eu}, \text{Yb}$ ) with  $\text{HSeSi}(\text{SiMe}_3)_3$  in hexanes or benzene- $d_6$  proceeded rapidly upon mixing, but complicated mixtures of uncharacterized products were formed. While some  $[\text{SeSi}(\text{SiMe}_3)_3]_2$  was seen in the  $^1\text{H}$  and  $^{13}\text{C}\{^1\text{H}\}$  NMR spectra, this was not the only byproduct. Reduction to the divalent state might be expected in these cases; however, the reactions are obviously more complex than the simple one-electron redox process suggested by eq 2.



The coordinatively unsaturated metal centers in the homoleptic complexes rapidly add Lewis bases to form adducts that are more stable, easier to isolate, and display higher crystallinity than their precursors. They were prepared directly by protonolysis of  $\text{Ln}[\text{N}(\text{SiMe}_3)_2]_3$  ( $\text{Ln} = \text{La}, \text{Sm}, \text{Yb}$ ) using  $\text{HSeSi}(\text{SiMe}_3)_3$  in THF (eq 3).



Crystallization from hexanes or toluene gave needles of colorless **3**, orange **4**, and purple **5** in yields ranging from 50 to 80%. The compounds are air- and moisture-sensitive, but unlike **1** and **2**, they are stable for several weeks under dry nitrogen as solids at room temperature under normal lighting conditions. In benzene- $d_6$ , **3** and **4** show no change by  $^1\text{H}$  NMR spectroscopy after 24 h at 115 °C in sealed tubes. Under the same conditions, **5** undergoes complete decomposition to a complex mixture of  $[\text{SeSi}(\text{SiMe}_3)_3]_2$ ,  $\text{Se}[\text{Si}(\text{SiMe}_3)_3]_2$ , and unidentified  $\text{SiMe}_3$ -containing products, with the sample remaining homogeneous.

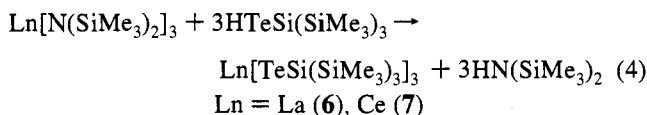
The  $^1\text{H}$  NMR spectrum of **3** shows two multiplets at 4.48 and 1.59 ppm and a singlet at 0.40 ppm in a 8:8:81 ratio,

indicating three equivalent selenolates and two equivalent THF ligands. Three singlets at 73.4, 25.4, and 0.98 ppm in the  $^{13}\text{C}\{^1\text{H}\}$  NMR spectrum confirm this assignment. No signals were observed in the  $^{77}\text{Se}\{^1\text{H}\}$  NMR spectrum in either benzene- $d_6$  or THF.

The  $^1\text{H}$  NMR spectra of **4** and **5** also suggest equivalent selenolate and equivalent THF ligands, but the peaks are shifted and broadened by the paramagnetic metal centers [**4**,  $\mu_{\text{eff}} = 1.8 \mu_{\text{B}}$ :  $\delta$  6.50 (8 H,  $\Delta\nu_{1/2} = 27 \text{ Hz}$ ), 2.63 (8 H,  $\Delta\nu_{1/2} = 15 \text{ Hz}$ ), 0.15 (s, 81 H); **5**,  $\mu_{\text{eff}} = 4.4 \mu_{\text{B}}$ :  $\delta$  7.35 (81 H,  $\Delta\nu_{1/2} = 62 \text{ Hz}$ ), -41.49 (8 H,  $\Delta\nu_{1/2} = 105 \text{ Hz}$ ), -72.80 (8 H,  $\Delta\nu_{1/2} = 197 \text{ Hz}$ )]. These magnetic moments fall in the ranges expected for trivalent Sm and Yb.<sup>22</sup> While no  $^{13}\text{C}\{^1\text{H}\}$  NMR signal is observed for **5**, **4** gives rise to only two singlets at 26.7 and 0.67 ppm. Comparison with the chemical shifts observed for **3** suggests that the missing third signal corresponds to the ether carbons, which should be closest to the paramagnetic center. No  $^{77}\text{Se}\{^1\text{H}\}$  NMR signals were detected. Unlike Sm and Yb, the analogous reaction of  $\text{Eu}[\text{N}(\text{SiMe}_3)_2]_3$  with 3 equiv of  $\text{HSeSi}(\text{SiMe}_3)_3$  and 2 equiv of THF in benzene- $d_6$  leads to a mixture of products.

No reaction was observed at 90 °C over more than 12 h between **3** and  $\text{H}_2$ , CO, 1-hexene, (trimethylsilyl)acetylene, dimethylacetylene,  $\text{P}^n\text{Bu}_3$ , or Te powder, as monitored by  $^1\text{H}$  NMR spectroscopy in benzene- $d_6$ . Complicated products form from reactions with  $^t\text{BuOO}^t\text{Bu}$ ,  $^t\text{BuSS}^t\text{Bu}$ ,  $\text{CO}_2$ ,  $\text{CS}_2$ , S powder,  $^t\text{BuNC}$ , or  $^t\text{BuOH}$ . The reaction of **3** with 3 equiv of MeI results in the slow quantitative formation of  $\text{MeSeSi}(\text{SiMe}_3)_3$  over the course of 24 h, while dry  $\text{O}_2$  reacts instantly to cleanly form  $[\text{SeSi}(\text{SiMe}_3)_3]_2$ . Coordination of  $\text{CH}_3\text{CN}$  occurs at room temperature, with no further reaction taking place over 12 h at 90 °C.

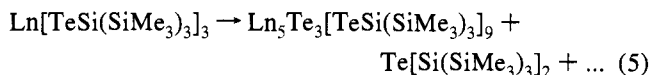
**Telluroolate Derivatives.** The tellurolysis reaction shown in eq 4 generates homoleptic trivalent lanthanide tellurolates in hydrocarbon solution.



NMR studies of the lanthanum reaction showed that the reaction is complete within a few minutes at room temperature. The amine byproduct appears to be coordinated at this point, but after about 2 h only free amine is observed along with signals we assign to base-free **6**. In benzene- $d_6$ , singlets appear in the  $^1\text{H}$ ,  $^{13}\text{C}\{^1\text{H}\}$ , and  $^{125}\text{Te}\{^1\text{H}\}$  NMR spectra at 0.55, 2.77, and 1018 ppm, respectively. NMR studies of **7** are less informative as the peaks are shifted and barely resolved from the base line due to paramagnetic coupling.

Attempts to isolate **6** and **7** as pure solids were fruitless due, for the most part, to the presence of impurities resulting from slow decomposition in solution. Over the course of 12 h at room temperature, the reaction mixture change in color from orange (**6**) and red (**7**) to dark brown. NMR spectra indicate the formation of a complicated mixture of  $\text{SiMe}_3$ -containing products, including  $\text{Te}[\text{Si}(\text{SiMe}_3)_3]_2$  and, to a lesser extent,  $[\text{TeSi}(\text{SiMe}_3)_3]_2$ , as the major components. When the volatiles from reactions carried out in benzene- $d_6$  were removed under vacuum within a few minutes, redissolution of the nonvolatile components indicated a mixture of unidentified products; neither starting material, product, nor any free or coordinated  $\text{HN}(\text{SiMe}_3)_2$  were present.

Although the homoleptic tellurolates could not be isolated from preparative scale reactions, these did lead to the isolation of interesting decomposition products, as shown below (eq 5).



Within a few minutes of mixing the tellurol and metal amides of La or Ce, the volatiles were removed under vacuum to yield dark brown solids. Upon dissolution in hexanes, thin needles began to precipitate after standing at room temperature, heating to reflux, or cooling to  $-40^\circ\text{C}$  overnight. These needles are insoluble in hydrocarbons and they decompose in polar solvents, preventing recrystallization and NMR studies. IR spectra indicate that the  $-\text{TeSi}(\text{SiMe}_3)_3$  ligand is present in these materials, but they provide little other information as to the nature of the species present.

Although most batches examined have been amorphous or weakly diffracting, one well-formed batch of needles was obtained from the cerium reaction that was suitable for study by X-ray crystallography.<sup>17</sup> The molecular structure of the cluster species obtained,  $\text{Ce}_5\text{Te}_3[\text{TeSi}(\text{SiMe}_3)_3]_9$  (**8**), is shown in Figure 3 with selected bond lengths and angles given in Table 2. This structure can be most easily viewed as a hexagonal ring of three  $[\text{TeCeTeR}]$  groups bridging through the telluride ligands, capped above and below by two bridging  $\text{Ce}(\text{TeR})_3$  groups. Alternatively, it can be thought of as a  $\text{Ce}_2\text{Te}_3$  core ( $\text{Ce}1$  and  $\text{Te}1$ ) surrounded by three bridging  $\text{Ce}(\text{TeR})_3$  groups. The  $\text{Ce}-\text{Te}$  bond lengths of 3.124(3) and 3.278(3) Å in the  $\text{Ce}_3\text{Te}_3$  ring are similar to those for the bridging tellurolates (3.183(2) and 3.235(1) Å) and substantially longer than those for the terminal ligands (3.026(3) Å). Bonding is evident between the capping cerium and ring telluride atoms, located 3.258(2) Å apart, with no other close inter- or intramolecular contacts. Predictions based on ionic radii yield bond lengths (3.10–3.22 Å)<sup>29,30</sup> that compare fairly well to the observed values, while poorer results are obtained from those based on covalent radii [3.01 Å (covalent), 2.94 Å (with ionic corrections)],<sup>31,32</sup> Few structures suitable for comparison exist (see below). The  $\text{Ce}-\text{Te}-\text{Si}$  angles are similar to those observed for related metal complexes of this ligand (typically  $120-130^\circ$ ),<sup>3,11,13,14</sup> with the bridging tellurolate being bent ( $\text{Ce}1-\text{Te}2-\text{Si}1$   $124.75(18)^\circ$  and  $\text{Ce}2-\text{Te}2-\text{Si}1$   $114.81(17)^\circ$ ) slightly more than the terminal ( $\text{Ce}2-\text{Te}3-\text{Si}5$   $132.4(3)^\circ$ ).

The elimination of  $\text{ER}_2$  ( $\text{E} = \text{chalcogen}$ ,  $\text{R} = \text{alkyl}$ ,  $\text{aryl}$ , or  $\text{silyl}$  group) from transition metal chalcogenolates is a well-documented mode of decomposition in the formation of metal chalcogenides,<sup>16,33–37</sup> but few examples of intermediates formed during these important transformations exist.<sup>11,12,14,38,39</sup> Although isolation of this compound provides one clue as to how these complicated reactions take place, there are clearly other unidentified species formed that may result from the same or related reactions (eq 5). Unfortunately, purification and characterization of these compounds has thus far been impossible. Attempts to prepare trivalent tellurolates of Sc and Y by similar methodology failed to yield any pure products.

(30) Bratsch, S. G.; Lagowski, J. J. *J. Phys. Chem.* **1985**, *89*, 3310. Tabulated values given are from references contained within.

(31) Porterfield, W. W. *Inorganic Chemistry, A Unified Approach*, 2nd ed.; Academic: New York, 1993; p 215.

(32) Emsley, J. *The Elements*, 2nd ed.; Clarendon: Oxford, 1991.

(33) Gindelberger, D. E.; Arnold, J. *Organometallics* **1994**, *13*, 4462.

(34) Arnold, J.; Walker, J. M.; Yu, K. M.; Bonasia, P. J.; Seligson, A. L.; Bourret, E. D. *J. Cryst. Growth* **1992**, *124*, 647.

(35) Brennan, J. G.; Slegrist, T.; Carroll, P. J.; Stuczynski, S. M.; Reynders, P.; Brus, L. E.; Steigerwald, M. L. *Chem. Mater.* **1990**, *2*, 403.

(36) Stuczynski, S. M.; Brennan, J. G.; Steigerwald, M. L. *Inorg. Chem.* **1989**, *28*, 4431.

(37) Steigerwald, M. L.; Sprinkle, C. R. *J. Am. Chem. Soc.* **1987**, *109*, 7200.

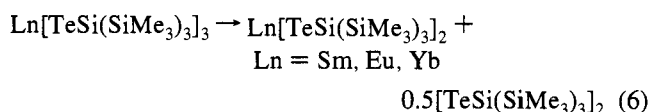
(38) Barron, A. R. *Chem. Soc. Rev.* **1993**, 93.

(39) Kraatz, H.-B.; Boorman, P. M.; Parvez, M. *Can. J. Chem.* **1993**, *71*, 1437.

**Table 1.** Crystallographic Data Collection Parameters for **8** and **9**

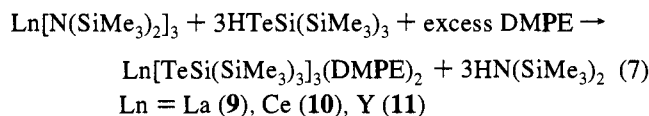
|                                    | <b>8</b>  | <b>9</b>   |
|------------------------------------|---|--|
| formula                            | $\text{Ce}_5\text{Te}_3\text{Si}_{12}\text{C}_8\text{H}_{24}$ | $\text{LaTe}_3\text{P}_4\text{Si}_{12}\text{C}_{39}\text{H}_{113}$ |
| mol weight                         | 4460.7  | 1565.0   |
| space group                        | $P6_3/m$  | $C2/c$   |
| $a/\text{Å}$                       | 20.456(5)   | 51.207(11)   |
| $b/\text{Å}$                       | 20.456(5)   | 15.725(3)  |
| $c/\text{Å}$                       | 28.063(9)   | 18.903(3)  |
| $\alpha/\text{deg}$                | 90  | 90   |
| $\beta/\text{deg}$                 | 90  | 92.698(15)   |
| $\gamma/\text{deg}$                | 120   | 90   |
| $\text{vol}/\text{Å}^3$            | 10170(8)  | 15204(9)   |
| $Z$                                | 2   | 8  |
| $d_{\text{calc}}/\text{g cm}^{-3}$ | 1.46  | 1.37   |
| crystal size/mm                    | $0.22 \times 0.29 \times 0.50$                                | $0.18 \times 0.25 \times 0.25$                                     |
| radiation ( $\lambda/\text{Å}$ )   | $\text{Mo K}\alpha$ (0.71073)                                 | $\text{Mo K}\alpha$ (0.71073)                                      |
| scan mode                          | $\omega$  |  |
| $2\theta$ range/deg                | 3–45  | 3–45   |
| collection range                   | $+h,+k,+l$  | $\pm h,+k,+l$  |
| absorption coeff, $\mu$            | 30.4  | 19.9   |
| no. of unique reflns               | 4539  | 9872   |
| reflns with $F^2 > 3\sigma(F^2)$   | 2607  | 6504   |
| final $R, R_w$                     | 0.061, 0.077  | 0.0374, 0.0373   |
| $T/^\circ\text{C}$                 | -103  | -110   |

Unlike the chemistry observed for the selenolates, reaction of  $\text{Ln}[\text{N}(\text{SiMe}_3)_2]_3$  ( $\text{Ln} = \text{Sm}, \text{Eu}, \text{Yb}$ ) with 3 equiv of  $\text{HTeSi}(\text{SiMe}_3)_3$  in hydrocarbons results in a clean reduction to divalent species, as shown by NMR spectroscopy and preparative scale reactions (eq 6).



This difference in reactivity can be ascribed to the greater reducing character of tellurolate anions compared to selenolates.<sup>40</sup> As we reported earlier, the reaction outlined in eq 6 provides a useful route to a series of divalent lanthanide tellurolates.<sup>3</sup>

Although the homoleptic tellurolates could not be isolated, addition of various Lewis bases gave isolable, well-characterized derivatives. For example, adducts **9–11** were prepared by the reaction of  $\text{Ln}[\text{N}(\text{SiMe}_3)_2]_3$  ( $\text{Ln} = \text{La}, \text{Ce}, \text{Y}$ ) and  $3\text{HTeSi}(\text{SiMe}_3)_3$  in the presence of DMPE in hexanes (eq 7).



NMR spectroscopy indicates quantitative conversion to products, and following preparative scale reactions, crystallization of **9–11** from hexanes gives bright yellow (**9**, **11**) or red (**10**) crystals in 70–90% yield.

These compounds are all air- and moisture-sensitive, but they show differing stability toward heat and vacuum. In the solid state, compound **9** decomposes after a few hours at room temperature and after a few minutes under vacuum, while both **10** and **11** are stable at room temperature under vacuum for a day or more. In solution, however, **9** and **10** both decompose rapidly above room temperature, while **11** shows only minor decomposition at  $100^\circ\text{C}$  for periods of less than 1 h (see below). As with the decomposition of the homoleptic species, the reactions are complex and mixtures of products are formed.

(40) Jensen, K. A.; Kjaer, A. In *The Chemistry of Organic Selenium and Tellurium Compounds*; Patal, S., Rappoport, Z., Eds.; Wiley: New York, 1986; Vol. 1, p 6.

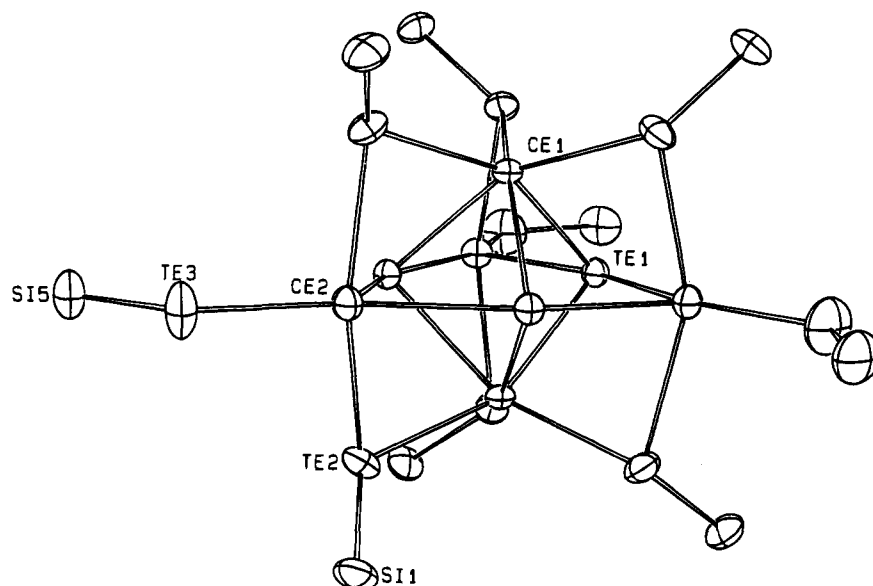


**Figure 3.** ORTEP view of  $\text{Ce}_5\text{Te}_3[\text{TeSi}(\text{SiMe}_3)_3]_9$  (**8**). Thermal ellipsoids are drawn at the 50% probability level with  $-\text{SiMe}_3$  groups omitted for clarity.

**Table 2.** Selected Bond Distances (Å) and Angles (deg) for **8**

|             |            |             |            |
|-------------|------------|-------------|------------|
| Ce1–Te1     | 3.258(2)   | Ce1–Te2     | 3.183(2)   |
| Ce2–Te1     | 3.124(3)   | Ce2–Te1     | 3.278(3)   |
| Ce2–Te2     | 3.235(1)   | Ce2–Te3     | 3.026(3)   |
| Te1–Ce1–Te1 | 79.39(5)   | Te1–Ce1–Te2 | 76.57(4)   |
| Te1–Ce1–Te2 | 86.69(4)   | Te1–Ce1–Te2 | 154.05(7)  |
| Te2–Ce1–Te2 | 111.37(4)  | Te1–Ce2–Te1 | 81.05(8)   |
| Te1–Ce2–Te2 | 77.74(4)   | Te1–Ce2–Te3 | 119.14(10) |
| Te1–Ce2–Te2 | 85.52(4)   | Te1–Ce2–Te3 | 159.81(10) |
| Te2–Ce2–Te2 | 154.90(8)  | Te2–Ce2–Te3 | 98.24(4)   |
| Ce1–Te1–Ce1 | 84.96(7)   | Ce1–Te1–Ce2 | 83.44(5)   |
| Ce1–Te1–Ce2 | 81.08(5)   | Ce2–Te1–Ce2 | 158.95(8)  |
| Ce1–Te2–Ce2 | 82.89(6)   | Ce1–Te2–Si1 | 124.75(18) |
| Ce2–Te2–Si1 | 114.81(17) | Ce2–Te3–Si5 | 132.4(3)   |

Few phosphine adducts of the lanthanides have been reported, supposedly due to the relatively weak interaction between these hard metals and soft bases.<sup>41</sup> We initially attempted to prepare derivatives with O- and N-donor ligands, but we found them less stable than complexes with phosphines. Both NMR and preparative studies showed that the protonolysis of  $\text{La}[\text{N}(\text{SiMe}_3)_2]_3$  with  $3\text{HTeSi}(\text{SiMe}_3)_3$  in the presence of THF, 1,2-dimethoxyethane, or pyridine led to bright yellow complexes that decomposed to dark orange-brown materials upon stirring for a few hours or removal of the volatiles under vacuum. These reactions were each examined using neat ligand as the solvent or a slight excess of ligand ( $\sim 4$  equiv) in hexanes or benzene- $d_6$ . The NMR spectra, color changes, and lack of solubility of the products formed in these reactions are similar to those observed in the decomposition of the homoleptic tellurolates in the presence of  $\text{HN}(\text{SiMe}_3)_2$ . In contrast, when TMEDA (TMEDA = 1,2-bis(dimethylamino)ethane) was used a bright yellow, crystalline compound was isolated, which we formulate as  $\text{La}[\text{TeSi}(\text{SiMe}_3)_3]_3(\text{TMEDA})_3$  based on  $^1\text{H}$  NMR data. All resonances were sharp at room temperature and indicated equivalent tellurolate and TMEDA ligands [ $\delta$  2.31 (s, 12 H), 2.08 (s, 36 H), 0.27 (s, 81 H)]. As with the DMPE adduct, however, this complex decomposes under dynamic vacuum by loss of base.

Compounds **9**–**11** crystallize readily from hexanes; one of these, the lanthanum derivative **9**, has been structurally characterized by X-ray crystallography.<sup>17</sup> A view of the molecule

is given in Figure 4 with selected bond lengths and angles in Table 3. Two tellurolates act as the axial ligands in a pseudopentagonal bipyramidal structure, with the DMPE ligands and one tellurolate in the equatorial plane. The La–Te bond lengths of 3.170(1), 3.168(1), and 3.141(1) Å fall in the range calculated by summation of ionic radii (3.13–3.24 Å);<sup>29,30</sup> predictions based on covalent radii are less accurate [3.05 Å (covalent), 2.98 Å (with ionic corrections)].<sup>31</sup> Two different sets of La–P bond lengths are observed, with the longer pair more nearly trans to the strongly donating equatorial tellurolate. There are no other structurally characterized lanthanum phosphine complexes for comparison, but the two sets of La–P bonds in **9** are approximately the same length as the Eu–P bond lengths measured for  $\{\text{Eu}[\text{TeSi}(\text{SiMe}_3)_3]_2(\text{DMPE})_2\}_2(\mu\text{-DMPE})_2$  (3.17 and 3.23 Å average for the chelating phosphines).<sup>3</sup> Differences in the ionic or covalent radii of lanthanum and europium predict that the Ln–P bonds should be about 0.1–0.2 Å longer for the europium complex.<sup>29,30,32</sup> Estimation of the Ln–P bond distances in other lanthanide phosphine complexes has also proven difficult.<sup>41</sup>

Steric effects are clearly important in defining the geometry of this complex. The three Te–La–Te angles of 145.69(2)°, 101.07(2)°, and 113.12(2)° indicate significant deviation from the idealized bipyramidal structure predicted from simple electrostatic considerations.<sup>42</sup> Presumably, the bulk of the  $-\text{Si}(\text{SiMe}_3)_3$  ligand is responsible for these deviations and also for the observation of two markedly different La–Te–Si angles (ca. 135–154°). Metrical parameters for the silyl groups and DMPE ligands are not unusual, and there are no unusually close inter- or intramolecular contacts.

The seven-coordinate solid-state structure is retained in solution as seen by NMR spectroscopy. All three DMPE derivatives are fluxional on the NMR time scale, with data for **11** being similar to that of **9** and **10**, but more informative. Thus, at 23 °C in toluene- $d_8$ , **11** shows broadened signals in the  $^1\text{H}$  NMR spectrum at 1.48, 1.43, and 0.36 ppm in the ratio 8:24:81. Combined with the observation of three broad peaks in the  $^{13}\text{C}\{^1\text{H}\}$  spectrum and a broad signal in the  $^{31}\text{P}\{^1\text{H}\}$  spectrum, these data indicate a stereochemically nonrigid structure in which the tellurolates and phosphines are rendered equivalent on the time scale of these NMR experiments. (No  $^{125}\text{Te}\{^1\text{H}\}$

(41) Fryzuk, M. D.; Haddad, T. S.; Berg, D. J. *Coord. Chem. Rev.* **1990**, *99*, 137.

(42) Kepert, D. L. *Prog. Inorg. Chem.* **1979**, *25*, 41.

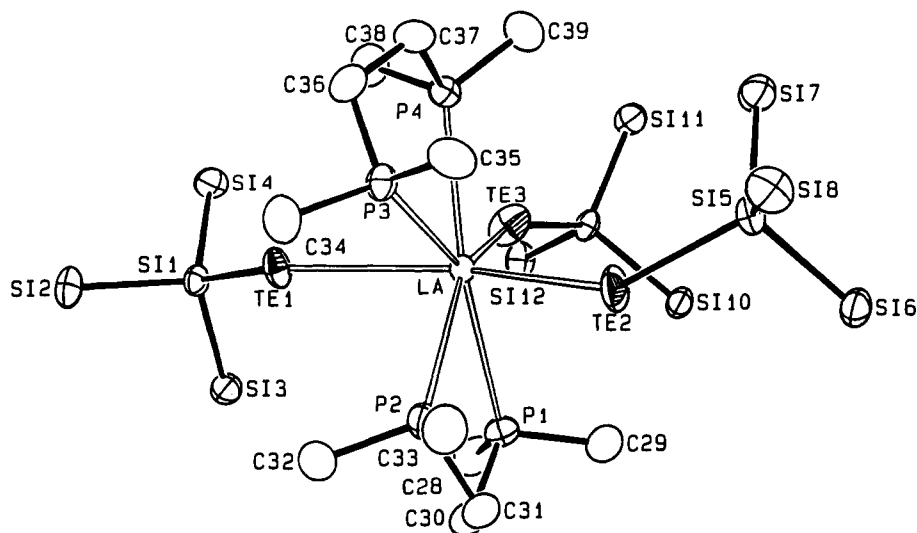


**Figure 4.** ORTEP view of  $\text{La}[\text{TeSi}(\text{SiMe}_3)_3]_3(\text{DMPE})_2$  (**9**). Thermal ellipsoids are drawn at the 50% probability level with  $-\text{SiMe}_3$  groups omitted for clarity.

**Table 3.** Selected Bond Distances (Å) and Angles (deg) for **9**

|            |           |            |           |
|------------|-----------|------------|-----------|
| La-Te1     | 3.170(1)  | La-Te2     | 3.168(1)  |
| La-Te3     | 3.141(1)  | La-P1      | 3.143(2)  |
| La-P2      | 3.208(2)  | La-P3      | 3.216(2)  |
| La-P4      | 3.127(2)  | Te1-La-Te2 | 145.69(2) |
| Te1-La-Te3 | 101.07(2) | Te2-La-Te3 | 113.12(2) |
| Te1-La-P1  | 101.32(4) | Te1-La-P2  | 82.21(4)  |
| Te1-La-P3  | 70.79(4)  | Te1-La-P4  | 83.86(4)  |
| Te2-La-P1  | 87.33(4)  | Te2-La-P2  | 71.85(4)  |
| Te2-La-P3  | 81.12(4)  | Te2-La-P4  | 102.22(4) |
| Te3-La-P1  | 81.05(4)  | Te3-La-P4  | 73.93(4)  |
| P1-La-P2   | 63.97(6)  | P2-La-P3   | 75.73(6)  |
| P3-La-P4   | 65.22(6)  | La-Te1-Si1 | 134.89(5) |
| La-Te2-Si5 | 142.34(6) | La-Te3-Si9 | 154.23(5) |

NMR signals could be detected.) Cooling the sample to  $-50$  °C results in the splitting and sharpening of these resonances. The  $^1\text{H}$  and  $^{13}\text{C}\{^1\text{H}\}$  NMR spectra each contain two singlets in the ratio 1:2, corresponding to inequivalent tellurolates (0.51, 0.38 ppm; 2.40, 1.68 ppm; respectively). A complicated  $^{31}\text{P}\{^1\text{H}\}$  NMR spectrum is observed, showing two multiplets in the ratio 1:1 at  $-26.3$  and  $-35.6$  ppm (Figure 5). Resolution enhancement and simulation of this spectrum as an AA'MM'X system ( $^{31}\text{P}$  and  $^{89}\text{Y}$  coupling) gave the coupling constants illustrated in Figure 6.<sup>43</sup> These values closely match those calculated by Fryzuk and co-workers for two yttrium-phosphine complexes with the same spin system.  $\text{Y}(\text{X})[\text{N}(\text{SiMe}_2\text{CH}_2\text{PMe}_2)_2]_2$  ( $\text{X} = \text{Cl}, \text{Ph}$ ).<sup>44</sup> The assignments of the  $\text{P}_i$  and  $\text{P}_c$  nuclei are based primarily on the  $\text{Y}-\text{P}$  coupling constants. The larger coupling is expected to be found for the  $\text{P}_i$  nuclei nearly trans to the electron donating tellurolate, with the cisoid  $\text{P}_c$  nuclei exhibiting smaller coupling. Previously observed  $|^1J_{\text{Y}-\text{P}}|$  of 59 Hz for  $\text{Y}(\text{OC}^i\text{Bu}_2\text{CH}_2\text{PMe}_2)_3$ <sup>45</sup> and 36–70 Hz for  $\text{Y}(\text{X})[\text{N}(\text{SiMe}_2\text{CH}_2\text{PMe}_2)_2]_2$  ( $\text{X} = \text{Cl}, \text{Ph}$ ) and  $\text{Y}(\text{Cl})[\text{N}(\text{SiMe}_2\text{CH}_2\text{PPh}_2)_2]_2$  compare favorably with the values of 40.6 and 63.2 Hz found here. In addition, the transoid  $\text{P}_c-\text{P}_c$  and  $\text{P}_i-\text{P}_c$  couplings are larger than the cisoid  $\text{P}_i-\text{P}_i$  and  $\text{P}_i-\text{P}_c$  interactions, as expected. As there are few known  $\text{Y}-\text{P}$  and  $\text{P}-\text{P}$  coupling constants in related species, further interpretation of these values would be premature. This spectrum, combined with inequivalent DMPE

methyl resonances in the  $^1\text{H}$  and  $^{13}\text{C}\{^1\text{H}\}$  NMR spectra (1.61, 1.12 ppm; 16.7, 15.5 ppm; respectively), indicate inequivalent  $\text{P}$ 's at low temperature.

Small satellites are observed in the low-temperature  $^{31}\text{P}\{^1\text{H}\}$  NMR spectrum, due to coupling from  $^{125}\text{Te}$  ( $I = 1/2$ , 7.0%). Coupling is only observed for the  $\text{P}_i$  resonance ( $|^2J_{\text{Te}-\text{P}}| = 105$  Hz), with the remaining satellites presumably overlapping the more intense, uncoupled transitions. The broadness observed in these satellites is also reflected in the  $^{125}\text{Te}\{^1\text{H}\}$  NMR spectrum at  $-50$  °C (Figure 7), a factor which prevents the unequivocal assignment of all the possible couplings. Further cooling in toluene- $d_8$  or pentane only broadens these signals. Even after resolution enhancement of the two broadened multiplets at  $-1031$  and  $-1198$  ppm (ratio 2:1, respectively), the apparent  $\Delta\nu_{1/2}$  for the upfield signals is 36 Hz and that for the downfield multiplet is 101 Hz. This triplet can be assigned to the equatorial tellurolate, coupled to  $\text{P}_i$  and  $\text{P}_i'$  only ( $|^2J_{\text{Te}-\text{P}}| = 105$  Hz), which is shifted to higher field due to transoid phosphorus nuclei. Coupling to  $\text{P}_c$ ,  $\text{P}_c'$ , and one  $\text{P}_i$  ( $|^2J_{\text{Te}-\text{P}}| \sim 105$  Hz for all three) presumably gives rise to the quartet at  $-1031$  ppm. Although little is known about  $\text{Te}-\text{P}$  coupling constants and  $\text{Te}-\text{Y}$  coupling constants have not been reported,  $|^2J_{\text{Te}-\text{P}}|$  values of 166, 80, and 78 Hz have been measured for  $\text{Zr}(\text{Te})[\text{TeSi}(\text{SiMe}_3)_3]_2(\text{DMPE})_2$ ,<sup>11</sup>  $\text{Fe}[\text{TeSi}(\text{SiMe}_3)_3]_2(\text{DMPE})_2$ , and  $\text{Fe}(\text{Cl})[\text{TeSi}(\text{SiMe}_3)_3]_3(\text{DMPE})_2$ .<sup>15</sup> Resolved coupling to three phosphorus nuclei for the pseudoaxial ligands suggests that the solution structure of **11** has 2-fold symmetry along the unique  $\text{La}-\text{Te}$  axis, but no mirror symmetry ( $C_2$  instead of  $C_{2v}$ ). Consideration of the  $\text{Te}_{\text{axial}}-\text{La}-\text{P}$  angles in the solid-state structure of **9** supports this interpretation, as  $\text{Te1}$  is bent back toward  $\text{P3}$  and  $\text{Te2}$  toward  $\text{P2}$  with respect to the  $\text{P1}-\text{P4}$  plane. This interpretation of the  $^{125}\text{Te}\{^1\text{H}\}$  NMR spectrum is incomplete but, at the very least, these data confirm the presence of inequivalent tellurolates in the ratio 2:1 at low temperature (no separation of the low-field multiplet into two multiplets is observed at other magnetic field strengths).

On warming **11** to  $80$  °C, partial sample decomposition occurs during the experiment (about 5%), but useful NMR spectra are still obtained. Singlets are found in both  $^1\text{H}$  and  $^{13}\text{C}\{^1\text{H}\}$  NMR spectra for the equivalent tellurolate ligands (0.33 and 2.30 ppm, respectively) and the equivalent DMPE methyl groups (1.47 and 17 ppm). The  $^{31}\text{P}\{^1\text{H}\}$  NMR spectrum shows a broad doublet (32.8 ppm,  $|^1J_{\text{PY}}| = 52$  Hz) flanked by  $^{125}\text{Te}$  satellites ( $|^2J_{\text{PTe}}| = 78$  Hz). Heating to higher temperatures only resulted

(43) Simulations were performed using the program NUMMARIT by R. A. Sebastian of the University of Manitoba, Winnipeg, Canada.

(44) Fryzuk, M. D.; Haddad, T. S.; Rettig, S. J. *Organometallics* **1991**, *10*, 2026.

(45) Hitchcock, P. B.; Lappert, M. F.; MacKinnon, I. A. *J. Chem. Soc., Chem. Commun.* **1988**, 1557.

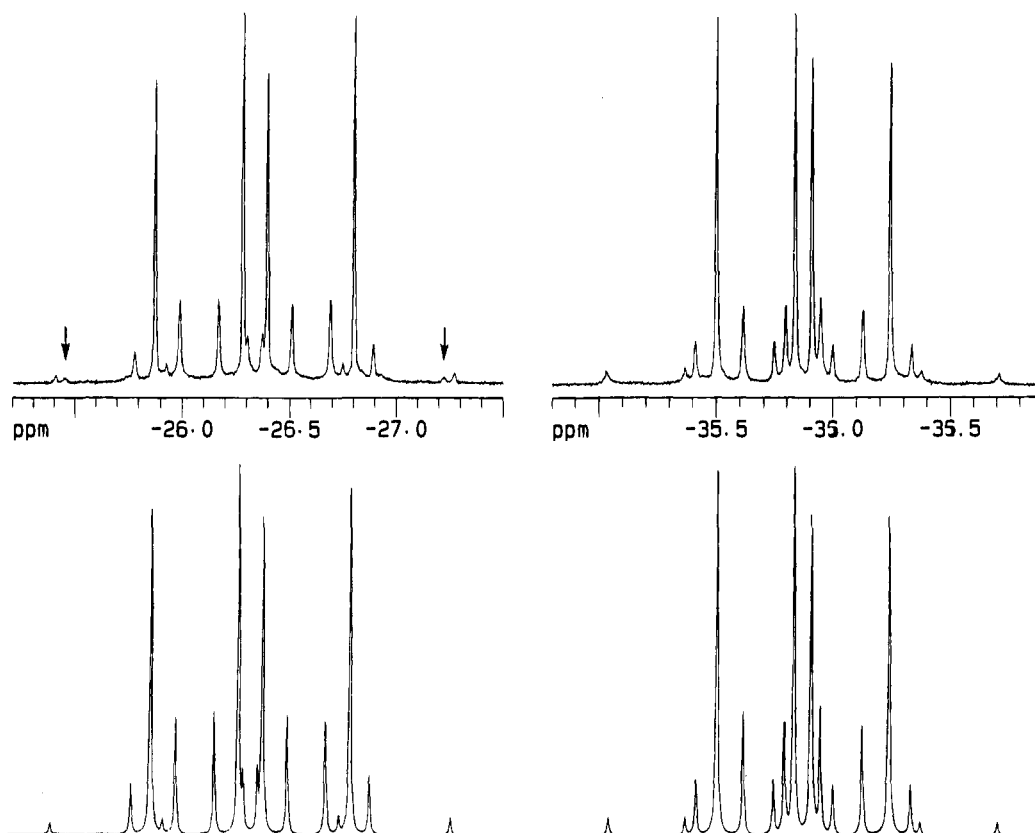


Figure 5. Experimental (above) and simulated (below)  $^{31}\text{P}\{^1\text{H}\}$  NMR spectra of  $\text{Y}[\text{TeSi}(\text{SiMe}_3)_3](\text{DMPE})_2$  (**11**) at  $-50\text{ }^\circ\text{C}$ .  $^{125}\text{Te}$  satellites are indicated by arrows.

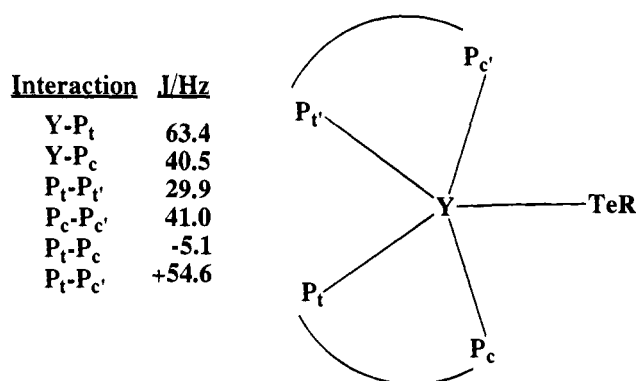


Figure 6.  $^2J_{\text{PP}}$  and  $^1J_{\text{PY}}$  for the  $^{31}\text{P}\{^1\text{H}\}$  NMR spectrum of  $\text{Y}[\text{TeSi}(\text{SiMe}_3)_3](\text{DMPE})_2$  (**11**) at  $-50\text{ }^\circ\text{C}$  (in Hz). The only sign specifications indicated by simulations is that the signs of the  $\text{P}_t-\text{P}_c$  and  $\text{P}_t'-\text{P}_c'$  couplings are opposite.

in further broadening of the peaks. These data indicate that **11** is close to the fast exchange limit, in which the tellurolates are equivalent and the phosphines are equivalent. Each coupling constant is the average of those observed at  $-50\text{ }^\circ\text{C}$ . Slight broadening of the peaks at this temperature ( $\Delta\nu_{1/2} = 20\text{ Hz}$ ) may result from decomposition of the sample and exchange with unbound DMPE produced by the decomposition.

About 3% uncoordinated DMPE is observed in the  $^{31}\text{P}\{^1\text{H}\}$  NMR spectrum of freshly recrystallized samples of **11** at room temperature. This peak is slightly broadened at room temperature ( $\Delta\nu_{1/2} = 21\text{ Hz}$ ) and sharp at  $-50\text{ }^\circ\text{C}$  ( $\Delta\nu_{1/2} = 6\text{ Hz}$ ), indicating slow exchange. The addition of free DMPE at room temperature does not reduce the line width of the  $^{31}\text{P}\{^1\text{H}\}$  NMR signal due to **11**. At  $80\text{ }^\circ\text{C}$ , the amount of uncoordinated DMPE increases to 10% and the line width of its signal increases to  $\Delta\nu_{1/2} = 104\text{ Hz}$ . These data indicate intermolecular exchange of DMPE; however, the rate of exchange is not fast enough to

account for the stereochemical nonrigidity of **11** ( $\Delta\nu_{1/2} = 534\text{ Hz}$  in the  $^{31}\text{P}\{^1\text{H}\}$  spectrum at room temperature), thus ruling out a process involving complete dissociation of phosphine.

To further investigate the nature of this fluxional process, the low-temperature  $^{89}\text{Y}$  EXSY spectrum was measured (Figure 8). The 1D  $^{89}\text{Y}$  NMR spectrum at  $-50\text{ }^\circ\text{C}$  consists of a low-field triplet of triplets at 592 ppm, with P–Y coupling matching that obtained from the simulation of the low-temperature  $^{31}\text{P}\{^1\text{H}\}$  NMR spectrum above (no  $^{125}\text{Te}$  coupling is observed). Cross peaks observed in the  $^{89}\text{Y}$  EXSY spectrum indicate that rearrangement of the phosphine ligands results in the interchange of  $\text{P}_c$  and  $\text{P}_t$  in only one of the DMPE ligands (making  $\text{P}_c$  chemically equivalent to  $\text{P}_t'$  and  $\text{P}_t$  chemically equivalent to  $\text{P}_c'$ ). Whether the DMPE ligands remain coordinated during this exchange or dissociate at one end is uncertain. The absence of  $^{125}\text{Te}$  coupling in this spectrum and broad peaks observed in the  $^{125}\text{Te}\{^1\text{H}\}$  EXSY spectrum (as in the 1D spectrum) prevent conclusive determination of how the tellurolate ligands exchange. Since the exchanges of the P nuclei and the Te nuclei occur at similar rates, this suggests that one process may simultaneously result in both exchanges. Due to the lability of the phosphine ligands observed in these and other complexes,<sup>44</sup> one reasonable explanation for ligand exchange involves a mechanism whereby one end of a DMPE ligand dissociates, giving a six-coordinate intermediate; ligand isomerization via a rhombic- or trigonal-twist,<sup>46</sup> followed by recoordination of the free DMPE phosphorus, would then render the three tellurolates and the two DMPE ligands equivalent.

## Experimental Section

**General.** Standard air- and moisture-sensitive techniques were used as previously described.<sup>9</sup> The compounds  $\text{Ln}[\text{N}(\text{SiMe}_3)_2]_3$  ( $\text{Ln} = \text{La}$ ,

(46) Huheey, J. E.; Keiter, E. A.; Keiter, R. L. *Inorganic Chemistry*, 4th ed.; Harper-Collins: New York, 1993.

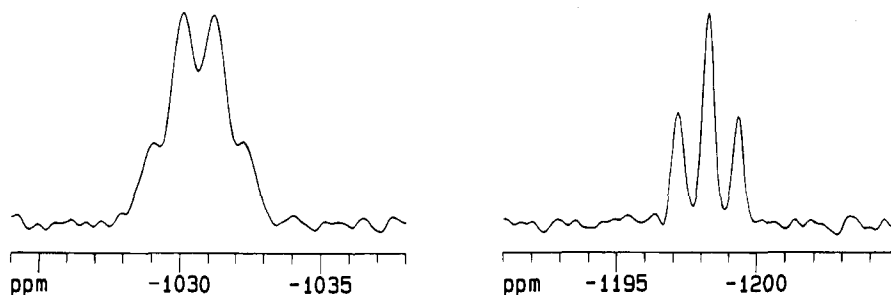


Figure 7.  $^{125}\text{Te}\{^1\text{H}\}$  NMR spectrum of  $\text{Y}[\text{TeSi}(\text{SiMe}_3)_3]_3(\text{DMPE})_2$  (**11**) at  $-50\text{ }^\circ\text{C}$ .

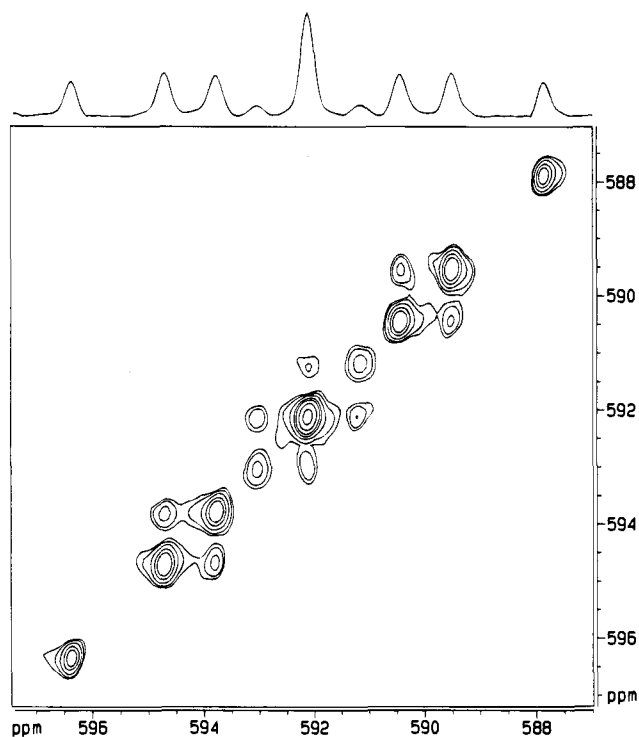


Figure 8.  $^{89}\text{Y}$  EXSY spectrum of  $\text{Y}[\text{TeSi}(\text{SiMe}_3)_3]_3(\text{DMPE})_2$  (**11**) at  $-36\text{ }^\circ\text{C}$  (64 ms mixing time). The vertical projection shows the normal 1D spectrum.

$\text{Sm}$ ,  $\text{Yb}$ ),<sup>27,47</sup>  $\text{HESi}(\text{SiMe}_3)_3$  ( $\text{E} = \text{Se}$ ,  $\text{Te}$ ),<sup>8</sup> and  $\text{DMPE}$ <sup>48</sup> were prepared by literature methods. Melting points were determined in capillaries sealed under  $\text{N}_2$  and are uncorrected. Samples for FT IR spectroscopy were prepared as Nujol mulls between KBr plates. All magnetic susceptibilities are corrected for the underlying diamagnetic susceptibility.<sup>49</sup> Elemental analyses were performed at the microanalytical laboratory in the College of Chemistry, University of California, Berkeley, CA.

**NMR Spectroscopy.** Unless otherwise stated, all NMR spectra were recorded at 300 MHz for  $^1\text{H}$ , 75.5 MHz for  $^{13}\text{C}$ , 121 MHz for  $^{31}\text{P}$ , 57.2 MHz for  $^{77}\text{Se}$ , 94.7 MHz for  $^{125}\text{Te}$ , and 24.5 MHz for  $^{89}\text{Y}$  at  $20\text{--}25\text{ }^\circ\text{C}$  using  $\text{C}_6\text{D}_6$  as the solvent. For  $^{89}\text{Y}$  only, a 10 mm probe was used (all others, 5 mm). Chemical shifts for  $^1\text{H}$  NMR spectra are relative to tetramethylsilane and were calibrated by measurement of the chemical shifts of the residual protons in the deuterated solvents used. Chemical shifts for  $^{13}\text{C}\{^1\text{H}\}$  NMR spectra are relative to tetramethylsilane and were calibrated by measurement of the chemical shifts of the deuterated solvents. Chemical shifts for  $^{31}\text{P}\{^1\text{H}\}$  NMR spectra are relative to external 85%  $\text{H}_3\text{PO}_4$  in  $\text{H}_2\text{O}$ . Chemical shifts for  $^{77}\text{Se}\{^1\text{H}\}$  NMR spectra are relative to  $\text{Me}_2\text{Se}$  and were calibrated with external 0.5 M  $\text{KSeCN}$  in ethanol ( $\delta$ -322 ppm). Chemical shifts for  $^{125}\text{Te}\{^1\text{H}\}$  NMR spectra are relative to  $\text{Me}_2\text{Te}$  and were calibrated with external 1.7 M

$\text{Te}(\text{OH})_6$  ( $\delta$  712 ppm). Chemical shifts for  $^{89}\text{Y}$  NMR spectra are relative to external 3.0 M  $\text{YCl}_3$  in  $\text{D}_2\text{O}$ . Average acquisition parameters for the  $^{89}\text{Y}$  NMR spectra of **2** and **11** were as follows: sample concentration, 0.2 M; acquisition time, 1.0 s; recycle delay, 0.05 s; pulse width,  $40\text{ }\mu\text{s}$  ( $90^\circ$  pulse at low temperature); sweep width, 5000 Hz; total data points, 4096; number of scans, 3000 (signals appeared in  $<20$  scans).

**$\text{La}[\text{SeSi}(\text{SiMe}_3)_3]_3$  (**1**).** Adding 20 mL of hexanes to a flask containing  $\text{La}[\text{N}(\text{SiMe}_3)_2]_3$  (289 mg, 0.466 mmol) and  $\text{HSeSi}(\text{SiMe}_3)_3$  (456 mg, 1.39 mmol) resulted in the immediate formation of clear yellow solution. After 10 min of stirring, the volatiles were removed under vacuum. Extraction of the resulting pale yellow powder with 10 mL of hexanes, followed by concentration of 3 mL and cooling to  $-40\text{ }^\circ\text{C}$ , yielded a pale yellow powder of **1** (234 mg, 43%) that typically co-crystallizes with 0.5 equiv of *n*-hexane that cannot be removed under prolonged vacuum. Anal. Calcd for  $\text{C}_{27}\text{H}_{81}\text{LaSe}_3\text{Si}_{12}$ : C, 28.99; H, 7.30. Found: C, 29.60; H, 7.50. Mp  $278\text{--}279\text{ }^\circ\text{C}$ .  $^1\text{H}$  NMR ( $\text{C}_7\text{D}_8$ ,  $24\text{ }^\circ\text{C}$ ):  $\delta$  1.22 (m, 4 H), 0.89 (t, 3 H,  $^3J_{\text{HH}} = 6.8\text{ Hz}$ ), 0.46 (s, 81 H).  $^{13}\text{C}\{^1\text{H}\}$  NMR ( $\text{C}_7\text{D}_8$ ,  $24\text{ }^\circ\text{C}$ ):  $\delta$  32.0, 23.0, 14.3, 1.52.  $^{77}\text{Se}\{^1\text{H}\}$  NMR ( $\text{C}_7\text{D}_8$ ,  $24\text{ }^\circ\text{C}$ ):  $\delta$  537 ( $\Delta\nu_{1/2} = 8\text{ Hz}$ ). IR ( $\text{cm}^{-1}$ ): 1307 w, 1254 m, 1243 s, 860 s, 837 s, 743 w, 722 w, 689 m, 623 m.

**$\{\text{Y}[\text{SeSi}(\text{SiMe}_3)_3]_2[\mu\text{-SeSi}(\text{SiMe}_3)_3]_2$  (**2**).** The procedure followed was analogous to that for **1**. The reaction of  $\text{Y}[\text{N}(\text{SiMe}_3)_2]_3$  (466 mg, 0.817 mmol) and  $\text{HSeSi}(\text{SiMe}_3)_3$  (803 mg, 2.45 mmol) gave a pale yellow powder of **2** (542 mg, 62%). Anal. Calcd for  $\text{C}_{27}\text{H}_{81}\text{Se}_3\text{Si}_{12}\text{Y}$ : C, 30.34; H, 7.64. Found: C, 29.90; H, 7.79. Mp  $280\text{--}281\text{ }^\circ\text{C}$ .  $^1\text{H}$  NMR ( $\text{C}_7\text{D}_8$ ,  $22\text{ }^\circ\text{C}$ ):  $\delta$  0.58 (s, 27 H,  $\Delta\nu_{1/2} = 9\text{ Hz}$ ), 0.40 (s, 54 H,  $\Delta\nu_{1/2} = 6\text{ Hz}$ ).  $^{13}\text{C}\{^1\text{H}\}$  NMR ( $\text{C}_7\text{D}_8$ ,  $22\text{ }^\circ\text{C}$ ):  $\delta$  2.60 ( $\Delta\nu_{1/2} = 9\text{ Hz}$ ), 1.38 ( $\Delta\nu_{1/2} = 4\text{ Hz}$ ).  $^{77}\text{Se}\{^1\text{H}\}$  NMR ( $\text{C}_7\text{D}_8$ ,  $22\text{ }^\circ\text{C}$ ):  $\delta$  -120 (t, 1 Se,  $|^1J_{\text{SeY}}| = 31\text{ Hz}$ ,  $\Delta\nu_{1/2} = 10\text{ Hz}$ ), -131 (d, 2 Se,  $|^1J_{\text{SeY}}| = 66\text{ Hz}$ ,  $\Delta\nu_{1/2} = 6\text{ Hz}$ ).  $^1\text{H}$  NMR ( $\text{C}_7\text{D}_8$ ,  $0\text{ }^\circ\text{C}$ ):  $\delta$  0.59 (s, 27 H,  $\Delta\nu_{1/2} = 4\text{ Hz}$ ), 0.41 (s, 54 H,  $\Delta\nu_{1/2} = 3\text{ Hz}$ ).  $^{13}\text{C}\{^1\text{H}\}$  NMR ( $\text{C}_7\text{D}_8$ ,  $0\text{ }^\circ\text{C}$ ):  $\delta$  2.54 ( $\Delta\nu_{1/2} = 3\text{ Hz}$ ), 1.29 ( $\Delta\nu_{1/2} = 2\text{ Hz}$ ).  $^{77}\text{Se}\{^1\text{H}\}$  NMR ( $\text{C}_7\text{D}_8$ ,  $0\text{ }^\circ\text{C}$ ):  $\delta$  -122 (t, 1 Se,  $|^1J_{\text{SeY}}| = 32\text{ Hz}$ ,  $\Delta\nu_{1/2} = 4\text{ Hz}$ ), -130 (d, 2 Se,  $|^1J_{\text{SeY}}| = 65\text{ Hz}$ ,  $\Delta\nu_{1/2} = 5\text{ Hz}$ ).  $^{89}\text{Y}$  NMR ( $\text{C}_7\text{D}_8$ ,  $0\text{ }^\circ\text{C}$ ):  $\delta$  995 (s,  $\Delta\nu_{1/2} = 3\text{ Hz}$ ,  $|^1J_{\text{SeY}}| = 32\text{ Hz}$ ,  $|^1J_{\text{SeY}}| = 65\text{ Hz}$ ).  $^1\text{H}$  NMR ( $\text{C}_7\text{D}_8$ ,  $100\text{ }^\circ\text{C}$ ):  $\delta$  0.43 (s,  $\Delta\nu_{1/2} = 12\text{ Hz}$ ).  $^{13}\text{C}\{^1\text{H}\}$  NMR ( $\text{C}_7\text{D}_8$ ,  $100\text{ }^\circ\text{C}$ ):  $\delta$  2.14 (s,  $\Delta\nu_{1/2} = 41\text{ Hz}$ ).  $^{77}\text{Se}\{^1\text{H}\}$  NMR ( $\text{C}_7\text{D}_8$ ,  $100\text{ }^\circ\text{C}$ ): no signal. IR ( $\text{cm}^{-1}$ ): 1396 m, 1310 w, 1242 s, 1196 w, 861 s, 836 s, 743 m, 723 w, 689 s, 624 s.

**$\text{La}[\text{SeSi}(\text{SiMe}_3)_3](\text{THF})_2$  (**3**).** Adding 25 mL of THF to a flask containing  $\text{La}[\text{N}(\text{SiMe}_3)_2]_3$  (568 mg, 0.916 mmol) and  $\text{HSeSi}(\text{SiMe}_3)_3$  (886 mg, 2.70 mmol) resulted in the immediate formation of a clear, colorless solution. After 20 min of stirring, the volatiles were removed under vacuum. Extraction of the resulting white powder with 50 mL of hexanes, followed by concentration and cooling to  $-40\text{ }^\circ\text{C}$ , yielded thin colorless needles of **3** (919 mg, 81%). Anal. Calcd for  $\text{C}_{35}\text{H}_{97}\text{LaO}_2\text{Se}_3\text{Si}_{12}$ : C, 33.29; H, 7.74. Found: C, 33.65; H, 7.89. Mp  $268\text{--}269\text{ }^\circ\text{C}$  dec.  $^1\text{H}$  NMR:  $\delta$  4.48 (m, 8 H), 1.59 (m, 8 H), 0.40 (s, 81 H).  $^{13}\text{C}\{^1\text{H}\}$  NMR:  $\delta$  73.4, 25.4, 0.98. IR ( $\text{cm}^{-1}$ ): 1307 w, 1257 m, 1242 s, 1018 m, 862 s, 834 s, 742 w, 719 w, 688 m, 623 m.

**$\text{Sm}[\text{SeSi}(\text{SiMe}_3)_3](\text{THF})_2$  (**4**).** The procedure followed was analogous to that for **3**. The reaction of  $\text{Sm}[\text{N}(\text{SiMe}_3)_2]_3$  (329 mg, 0.521 mmol) and  $\text{HSeSi}(\text{SiMe}_3)_3$  (511 mg, 1.56 mmol) gave orange needles of **4** (333 mg, 53%). Anal. Calcd for  $\text{C}_{35}\text{H}_{97}\text{O}_2\text{Se}_3\text{Si}_{12}\text{Sm}$ : C, 32.99; H, 7.67. Found: C, 32.93; H, 7.67. Mp  $237\text{--}241\text{ }^\circ\text{C}$  dec.  $\mu_{\text{eff}} = 1.8\text{ }\mu\text{B}$  (Evans' method),<sup>50</sup>  $^1\text{H}$  NMR:  $\delta$  6.50 (br, 8 H,  $\Delta\nu_{1/2} = 27\text{ Hz}$ ), 2.63 (br, 8 H,  $\Delta\nu_{1/2} = 15\text{ Hz}$ ), 0.15 (s, 81 H).  $^{13}\text{C}\{^1\text{H}\}$  NMR:  $\delta$  26.7, 0.67. IR ( $\text{cm}^{-1}$ ): 1308 w, 1257 m, 1242 s, 1034 w, 1016 m, 916 w, 861 s, 833 s, 743 w, 722 w, 688 s, 623 s.

(47) LaDuca, R. L.; Wolczanski, P. T. *Inorg. Chem.* **1992**, *31*, 1311.

(48) Burt, R. J.; Chatt, J.; Hussain, W.; Leigh, G. J. *J. Organomet. Chem.* **1979**, *182*, 203.

(49) Selwood, P. W. *Magnetochemistry* 2nd ed.; Interscience: New York, 1956.

(50) Evans, D. F.; James, T. A. *J. Chem. Soc., Dalton Trans.* **1979**, 723.



**Yb[SeSi(SiMe<sub>3</sub>)<sub>3</sub>]<sub>3</sub>(THF)<sub>2</sub> (5).** The procedure allowed was analogous to that for **3**. The reaction of Yb[N(SiMe<sub>3</sub>)<sub>2</sub>]<sub>3</sub> (251 mg, 0.384 mmol) and HSeSi(SiMe<sub>3</sub>)<sub>3</sub> (378 mg, 1.15 mmol) gave purple needles of **5** (358 mg, 72%). Anal. Calcd for C<sub>35</sub>H<sub>97</sub>O<sub>2</sub>Se<sub>3</sub>Si<sub>12</sub>Yb: C, 32.41; H, 7.54. Found: C, 32.44; H, 7.14. Mp 218–220 °C dec.  $\mu_{\text{eff}} = 4.4 \mu_{\text{B}}$  (Johnson-Matthey MSB-1 Evans' balance). <sup>1</sup>H NMR:  $\delta$  7.35 (s, 81 H,  $\Delta\nu_{1/2} = 62$  Hz), -41.49 (br, 8 H,  $\Delta\nu_{1/2} = 105$  Hz), -72.80 (br, 8 H,  $\Delta\nu_{1/2} = 197$  Hz). IR (cm<sup>-1</sup>): 1309 w, 1257 m, 1242 s, 1035 w, 1012 m, 919 w, 860 s, 835 s, 743 m, 723 w, 687 s, 624 s.

**Reaction of Ce[N(SiMe<sub>3</sub>)<sub>2</sub>]<sub>3</sub> with 3HTeSi(SiMe<sub>3</sub>)<sub>3</sub>.** Adding a solution of Ce[N(SiMe<sub>3</sub>)<sub>2</sub>]<sub>3</sub> (311 mg, 0.501 mmol) in 20 mL of hexanes to a solution of HTeSi(SiMe<sub>3</sub>)<sub>3</sub> (566 mg, 1.50 mmol) in 20 mL of hexanes resulted in the immediate formation of a clear, deep red solution that slowly turned darker over the next few minutes. After 15 min of stirring, removal of the volatiles under vacuum left a red-brown solid that was extracted with 20 mL of hexanes. Concentration resulted in the precipitation of a fine red crystalline precipitate, which did not redissolve with the addition of more solvent or gentle warming. Attempts to recrystallize the recovered solid resulted in product decomposition. The highest yields of material were obtained by allowing the reaction mixture to sit at room temperature for a few days (232 mg, 52% of the theoretical yield expected for Ce<sub>5</sub>Te<sub>3</sub>[TeSi(SiMe<sub>3</sub>)<sub>3</sub>]<sub>9</sub>). Thin needles suitable for X-ray crystallography were obtained by cooling the hexanes extract of the reaction mixture to -40 °C. Anal. Calcd for C<sub>81</sub>H<sub>243</sub>Ce<sub>5</sub>Si<sub>36</sub>Te<sub>12</sub>: C, 21.81; H, 5.49. Found: C, 24.69; H, 6.10. IR (cm<sup>-1</sup>): 1306 w, 1256 w, 858 m, 836 s, 746 w, 735 w, 722 w, 689 m, 623 m.

**Reaction of La[N(SiMe<sub>3</sub>)<sub>2</sub>]<sub>3</sub> with 3HTeSi(SiMe<sub>3</sub>)<sub>3</sub>.** The procedure followed was the same as that for Ce[N(SiMe<sub>3</sub>)<sub>2</sub>]<sub>3</sub> with 3 equiv of HTeSi(SiMe<sub>3</sub>)<sub>3</sub>. The reaction of La[N(SiMe<sub>3</sub>)<sub>2</sub>]<sub>3</sub> (903 mg, 1.46 mmol) with HTeSi(SiMe<sub>3</sub>)<sub>3</sub> (1.65 g, 4.38 mmol) gave a fine orange crystalline precipitate (816 mg, 63% of the theoretical yield expected for La<sub>5</sub>Te<sub>3</sub>[TeSi(SiMe<sub>3</sub>)<sub>3</sub>]<sub>9</sub>). Elemental analysis was not attempted due to sample inhomogeneity. X-ray powder diffraction showed only very weak diffraction patterns. IR (cm<sup>-1</sup>): 1244 s, 858 s, 832 s, 742 w, 688 m, 623 m.

**Reaction of Y[N(SiMe<sub>3</sub>)<sub>2</sub>]<sub>3</sub> with 3HTeSi(SiMe<sub>3</sub>)<sub>3</sub>.** The procedure followed was the similar to that for Ce[N(SiMe<sub>3</sub>)<sub>2</sub>]<sub>3</sub> with 3HTeSi(SiMe<sub>3</sub>)<sub>3</sub>, except that the reaction was stirred for 24 h. The reaction of Y[N(SiMe<sub>3</sub>)<sub>2</sub>]<sub>3</sub> (178 mg, 0.312 mmol) and HTeSi(SiMe<sub>3</sub>)<sub>3</sub> (351 mg, 0.933 mmol) followed by extraction with 10 mL of toluene gave a fine orange crystalline precipitate (100 mg, 38% of the theoretical yield expected for Y<sub>5</sub>Te<sub>3</sub>[TeSi(SiMe<sub>3</sub>)<sub>3</sub>]<sub>9</sub>). Recrystallization from toluene resulted in sample decomposition. Elemental analysis was not attempted due to sample inhomogeneity. IR (cm<sup>-1</sup>): 1255 w, 1243 m, 858 m, 836 s, 726 w, 689 w, 624 w.

**La[TeSi(SiMe<sub>3</sub>)<sub>3</sub>]<sub>3</sub>(DMPE)<sub>2</sub> (9).** Addition of HTeSi(SiMe<sub>3</sub>)<sub>3</sub> (1.663 g, 4.420 mmol) in 25 mL of hexanes to a solution of La[N(SiMe<sub>3</sub>)<sub>2</sub>]<sub>3</sub> (0.911 g, 1.47 mmol) and DMPE (0.52 mL, 3.1 mmol) in 25 mL of hexanes resulted in an immediate color change to bright yellow. After 15 min, the solvent was removed under vacuum to give a yellow solid. The solid was extracted with hexanes, filtered, concentrated, and cooled to -40 °C to give yellow crystals (1.96 g, 86%). Recrystallization from hexanes gave crystals suitable for X-ray diffraction. Anal. Calcd for C<sub>39</sub>H<sub>113</sub>LaP<sub>4</sub>Si<sub>12</sub>Te<sub>3</sub>: C, 29.93; H, 7.28. Found: C, 29.88; H, 7.35. Mp 230–232 °C dec. <sup>1</sup>H NMR (C<sub>7</sub>D<sub>8</sub>, 400 MHz, 23 °C):  $\delta$  1.46 (v br s, 8 H), 1.44 (s, 24 H,  $\Delta\nu_{1/2} = 6$  Hz), 0.45 (s, 81 H,  $\Delta\nu_{1/2} = 1$  Hz). <sup>13</sup>C{<sup>1</sup>H} NMR (C<sub>7</sub>D<sub>8</sub>, 23 °C):  $\delta$  32.0 ( $\Delta\nu_{1/2} = 3$  Hz), 16.1 ( $\Delta\nu_{1/2} = 9$  Hz), 1.80 ( $\Delta\nu_{1/2} = 3$  Hz). <sup>31</sup>P{<sup>1</sup>H} NMR (C<sub>7</sub>D<sub>8</sub>, 162 MHz, 23 °C):  $\delta$  -29.4 (s,  $\Delta\nu_{1/2} = 312$  Hz). <sup>125</sup>Te{<sup>1</sup>H} NMR (C<sub>7</sub>D<sub>8</sub>, 21 °C): no signal. <sup>1</sup>H NMR (C<sub>7</sub>D<sub>8</sub>, 400 MHz, -84 °C):  $\delta$  1.64 (s, 12 H,  $\Delta\nu_{1/2} = 10$  Hz), 1.13 (s, 12 H,  $\Delta\nu_{1/2} = 10$  Hz), 0.68 (s, 27 H,  $\Delta\nu_{1/2} = 6$  Hz), 0.52 (s, 54 H,  $\Delta\nu_{1/2} = 5$  Hz). <sup>13</sup>C{<sup>1</sup>H} NMR (C<sub>7</sub>D<sub>8</sub>, -84 °C):  $\delta$  32.4 ( $\Delta\nu_{1/2} = 3$  Hz), 23.4 ( $\Delta\nu_{1/2} = 3$  Hz), 16.3 ( $\Delta\nu_{1/2} = 14$  Hz), 14.8 ( $\Delta\nu_{1/2} = 3$  Hz), 1.81 ( $\Delta\nu_{1/2} = 5$  Hz), 1.44 ( $\Delta\nu_{1/2} = 4$  Hz). <sup>31</sup>P{<sup>1</sup>H} NMR (C<sub>7</sub>D<sub>8</sub>, 162 MHz, -84 °C):  $\delta$  -21.9 s, 1 P,  $\Delta\nu_{1/2} = 57$  Hz), -34.0 (s, 1 P,  $\Delta\nu_{1/2} = 49$  Hz). <sup>125</sup>Te{<sup>1</sup>H} NMR (C<sub>7</sub>D<sub>8</sub>, -70 °C):  $\delta$  -894 (s, 2 Te,  $\Delta\nu_{1/2} = 260$  Hz), -1074 (s, 1 Te,  $\Delta\nu_{1/2} = 125$  Hz). IR (cm<sup>-1</sup>): 1415 m, 1297 w, 1240 s, 945 m, 858 s, 833 s, 731 w, 688 m, 625 m.

**Ce[TeSi(SiMe<sub>3</sub>)<sub>3</sub>]<sub>3</sub>(DMPE)<sub>2</sub> (10).** The procedure followed was the same as that for **9**. The reaction of Ce[N(SiMe<sub>3</sub>)<sub>2</sub>]<sub>3</sub> (0.964 g, 1.55 mmol), HTeSi(SiMe<sub>3</sub>)<sub>3</sub> (1.76 g, 4.68 mmol), and DMPE (0.53 mL, 3.2

mmol) gave red crystals that were placed under vacuum overnight to give **10** (1.773 g, 73%) as a red powder. Prolonged evacuation was necessary to remove 1 equiv of co-crystallized *n*-hexane. Anal. Calcd for C<sub>39</sub>H<sub>113</sub>CeP<sub>4</sub>Si<sub>12</sub>Te<sub>3</sub>: C, 29.91; H, 7.27. Found: C, 29.87; H, 7.15. Mp 200–202 °C dec. <sup>1</sup>H NMR (C<sub>7</sub>D<sub>8</sub>, 400 MHz, 23 °C):  $\delta$  5.87 (s, 8 H,  $\Delta\nu_{1/2} = 30$  Hz), 4.07 (s, 24 H,  $\Delta\nu_{1/2} = 14$  Hz), -0.28 (s, 81 H,  $\Delta\nu_{1/2} = 32$  Hz). <sup>13</sup>C{<sup>1</sup>H} NMR (C<sub>7</sub>D<sub>8</sub>, 23 °C):  $\delta$  33.4 ( $\Delta\nu_{1/2} = 8$  Hz), 21.4 ( $\Delta\nu_{1/2} = 11$  Hz), 1.44 ( $\Delta\nu_{1/2} = 3$  Hz). <sup>31</sup>P{<sup>1</sup>H} NMR (C<sub>7</sub>D<sub>8</sub>, 23 °C): no signal. <sup>1</sup>H NMR (C<sub>7</sub>D<sub>8</sub>, 400 MHz, -78 °C):  $\delta$  11.45 (s, 4 H,  $\Delta\nu_{1/2} = 55$  Hz), 8.51 (s, 4 H,  $\Delta\nu_{1/2} = 59$  Hz), 7.65 (s, 12 H,  $\Delta\nu_{1/2} = 44$ ), 5.38 (s, 12 H,  $\Delta\nu_{1/2} = 36$  Hz), 1.16 (s, 27 H,  $\Delta\nu_{1/2} = 10$  Hz), -2.12 (s, 54 H,  $\Delta\nu_{1/2} = 8$  Hz). <sup>13</sup>C{<sup>1</sup>H} NMR (C<sub>7</sub>D<sub>8</sub>, -78 °C):  $\delta$  28.2 ( $\Delta\nu_{1/2} = 30$  Hz), 22.0, 3.08 ( $\Delta\nu_{1/2} = 8$  Hz), -1.17 ( $\Delta\nu_{1/2} = 4$  Hz). <sup>31</sup>P{<sup>1</sup>H} NMR (C<sub>7</sub>D<sub>8</sub>, -78 °C):  $\delta$  765.5 (s, 1P,  $\Delta\nu_{1/2} = 262$  Hz), 652.2 (s, 1P,  $\Delta\nu_{1/2} = 186$  Hz). IR (cm<sup>-1</sup>): 2361 w, 1923 w, 1860 w, 1420 m, 1295 w, 1278 w, 1253 m, 1240 s, 944 m, 929 m, 888 m, 861 s, 834 s, 734 w, 686 m, 624 m.

**Y[TeSi(SiMe<sub>3</sub>)<sub>3</sub>]<sub>3</sub>(DMPE)<sub>2</sub> (11).** The procedure followed was the same as that for **9**. The reaction of Y[N(SiMe<sub>3</sub>)<sub>2</sub>]<sub>3</sub> (1.02 g, 1.80 mmol), HTeSi(SiMe<sub>3</sub>)<sub>3</sub> (2.02 g, 5.37 mmol), and DMPE (1.2 mL, 7.2 mmol) gave yellow crystals (2.40 g, 89%). Anal. Calcd for C<sub>39</sub>H<sub>113</sub>P<sub>4</sub>Si<sub>12</sub>Te<sub>3</sub>Y: C, 29.93; H, 7.28. Found: C, 29.88; H, 7.35. Mp 152–153 °C dec. <sup>1</sup>H NMR (C<sub>7</sub>D<sub>8</sub>, 23 °C):  $\delta$  1.48 (s, 8H,  $\Delta\nu_{1/2} = 8$  Hz), 1.43 (s, 24 H,  $\Delta\nu_{1/2} = 12$  Hz), 0.36 (s, 81 H,  $\Delta\nu_{1/2} = 6$  Hz). <sup>13</sup>C{<sup>1</sup>H} NMR (C<sub>7</sub>D<sub>8</sub>, 23 °C):  $\delta$  26.4 (very broad, barely visible), 16.6 (m,  $\Delta\nu_{1/2} = 16$  Hz), 2.12 ( $\Delta\nu_{1/2} = 2$  Hz). <sup>31</sup>P{<sup>1</sup>H} NMR (C<sub>7</sub>D<sub>8</sub>, 23 °C):  $\delta$  -32.3 (s,  $\Delta\nu_{1/2} = 530$  Hz). <sup>125</sup>Te{<sup>1</sup>H} NMR (C<sub>7</sub>D<sub>8</sub>, 21 °C): no signal. <sup>1</sup>H NMR (C<sub>7</sub>D<sub>8</sub>, -50 °C):  $\delta$  1.61 (s, 12 H,  $\Delta\nu_{1/2} = 11$  Hz), 1.34 (br, 8 H,  $\Delta\nu_{1/2} = 36$  Hz), 1.12 (s, 12 H,  $\Delta\nu_{1/2} = 10$  Hz), 0.51 (s, 27 H,  $\Delta\nu_{1/2} = 5$  Hz), 0.38 (s, 54 H,  $\Delta\nu_{1/2} = 6$  Hz). <sup>13</sup>C{<sup>1</sup>H} NMR (C<sub>7</sub>D<sub>8</sub>, -50 °C):  $\delta$  28.0 (very broad, barely visible), 23.2 (very broad, barely visible), 16.7 ( $\Delta\nu_{1/2} = 10$  Hz), 15.5 ( $\Delta\nu_{1/2} = 17$  Hz), 2.40 ( $\Delta\nu_{1/2} = 2$  Hz), 1.68 ( $\Delta\nu_{1/2} = 2$  Hz). <sup>31</sup>P{<sup>1</sup>H} NMR (C<sub>7</sub>D<sub>8</sub>, -50 °C):  $\delta$  -26.3 (1P), -35.6 (1P), see discussion for coupling. <sup>125</sup>Te{<sup>1</sup>H} NMR (C<sub>7</sub>D<sub>8</sub>, -50 °C):  $\delta$  -1031 (2 Te), -1198 (1 Te), see discussion for coupling. <sup>89</sup>Y NMR (C<sub>7</sub>D<sub>8</sub>, -50 °C):  $\delta$  592 (tt,  $\Delta\nu_{1/2} = 5$  Hz,  $|^1J_{Y-P}| = 40.6$  Hz,  $|^1J_{Y-P}| = 63.2$  Hz). <sup>1</sup>H NMR (C<sub>7</sub>D<sub>8</sub>, 80 °C):  $\delta$  1.53 (br, 8 H,  $\Delta\nu_{1/2} = 21$  Hz), 1.47 (s, 24 H,  $\Delta\nu_{1/2} = 11$  Hz), 0.33 (s, 81 H,  $\Delta\nu_{1/2} = 2$  Hz). <sup>13</sup>C{<sup>1</sup>H} NMR (C<sub>7</sub>D<sub>8</sub>, 80 °C):  $\delta$  27.1 ( $\Delta\nu_{1/2} = 11$  Hz), 17.1 ( $\Delta\nu_{1/2} = 13$  Hz), 2.30 ( $\Delta\nu_{1/2} = 2$  Hz). <sup>31</sup>P{<sup>1</sup>H} NMR (C<sub>7</sub>D<sub>8</sub>, 80 °C):  $\delta$  -32.8 (d,  $\Delta\nu_{1/2} = 19$  Hz,  $|^1J_{PY}| = 52$  Hz,  $|^2J_{PTe}| = 34$  Hz). <sup>125</sup>Te{<sup>1</sup>H} NMR (C<sub>7</sub>D<sub>8</sub>, 80 °C): no signal. IR (cm<sup>-1</sup>): 1420 w, 1299 w, 1290 w, 1277 w, 1254 m, 1239 s, 1135 w, 1088 w, 1001 w, 948 m, 930 m, 888 m, 861 s, 836 s, 736 w, 727 w, 685 s, 644 w, 623 s.

**X-ray Crystallography.** Table 1 contains details of crystal and data collection parameters. The structures of **8** and **9** were determined by Dr. F. J. Hollander at the CHEXRAY crystallographic facility in the College of Chemistry, University of California, Berkeley.

**8.** Small dark red needles were obtained by slow crystallization from a hexanes solution at -40 °C. A suitable fragment was cleaved and mounted on a glass fiber using Paratone N hydrocarbon oil. The crystal was transferred to an Enraf-Nonius CAD-4 diffractometer, centered in the beam, and cooled to -103 °C. Automatic peak search and indexing procedures followed by inspection of the systematic absences indicated the space group *P6<sub>3</sub>/m*.

The 4998 raw intensity data were converted to structure factor amplitudes and their esd's by correction for scan speed, background, and Lorentz and polarization effects. Intensity standards were measured on the diffractometry every 1 h of data collection and did not decrease significantly over the data collection period. Three reflections were checked after every 250 measurements as orientation checks. Crystal orientation was redetermined if any of the reflections were offset by more than 0.10° from their predicted positions. Inspection of the azimuthal scan data showed a variation  $I_{\text{min}}/I_{\text{max}} = 0.67$  for the average curve. An empirical correction based on the observed variation was applied to the data. Removal of systematic absences left 4539 unique reflections.

The crystal structure was solved using direct methods (SHELXS-86)<sup>51</sup> and refined by standard least-squares and Fourier techniques.

(51) Sheldrick, G. M. *Crystallographic Computing 3*; Oxford University Press: Oxford, 1985; p 175.

Following refinement of all non-hydrogen atoms with anisotropic thermal parameters, all hydrogen atoms were assigned idealized positions. They were included in the structure factor calculations, but not refined.

The final residuals for 144 variables against the 2607 data for which  $F^2 > 3\sigma(F^2)$  were  $R = 0.061$ ,  $R_w = 0.077$ , and  $GOF = 2.22$ . The  $R$  value for all 4539 data was 0.114. The largest peak in the final difference Fourier map had an electron density of  $+1.86 \text{ e}^-/\text{\AA}^3$  and the lowest excursion  $-0.29 \text{ e}^-/\text{\AA}^3$ .

Refinement in the acentric space group  $P6_3$  was tested, but it gave no better agreement than refinement in the centric group with disorder of the  $\text{Si}(\text{SiMe}_3)_3$  groups partially modeled. The heavy atoms in the structure were well-ordered.

9. Large yellow plates were obtained by slow crystallization from a saturated hexanes solution at  $-40 \text{ }^\circ\text{C}$ . A suitable fragment was cleaved and mounted on a glass fiber using Paratone N hydrocarbon oil. The crystal was transferred to an Enraf-Nonius CAD-4 diffractometer, centered in the beam, and cooled to  $-110 \text{ }^\circ\text{C}$ . Automatic peak search and indexing procedures followed by inspection of the systematic absences indicated the space groups  $Cc$  or  $C2/c$ .

The 10655 raw intensity data were converted to structure factor amplitudes and their esd's by correction for scan speed, background, and Lorentz and polarization effects. Intensity standards were measured on the diffractometer every 1 h of data collection and showed a 6% decrease in intensity over the data collection period. The data were corrected for this decay. Three reflections were checked after every 200 measurements as orientation checks. Crystal orientation was redetermined if any of the reflections were offset by more than  $0.10^\circ$  from their predicted positions; such orientation was necessary two times during data collection. Inspection of the azimuthal scan data showed a variation  $I_{\text{min}}/I_{\text{max}} = 0.86$  for the average curve. An empirical correction based on the observed variation was applied to the data. The choice of the centric space group  $C2/c$  was confirmed by the successful solution and refinement of the structure.

The crystal structure was solved using direct methods (SHELXS-86)<sup>51</sup> and refined by standard least-squares and Fourier techniques. Following refinement of all non-hydrogen atoms with anisotropic thermal parameters, all hydrogen atoms were assigned idealized positions. They were included in the structure factor calculations, but not refined.

The final residuals for 532 variables against the 6504 data for which  $F^2 > 3\sigma(F^2)$  were  $R = 0.0374$ ,  $R_w = 0.0373$ , and  $GOF = 1.16$ . The  $R$  value for all 9872 data was 0.0753. The largest peak in the final difference Fourier map had an electron density of  $1.19 \text{ e}^-/\text{\AA}^3$  and the lowest excursion  $-0.16 \text{ e}^-/\text{\AA}^3$ . The largest peaks were all located near the La and Te atoms.

**Acknowledgment.** We are grateful to the National Science Foundation (CHE-9210406) for financial support, the Department of Education for a fellowship to D.R.C., and the Alfred P. Sloan Foundation for the award of a research fellowship to J.A. We also thank Mr. R. Nunlist for his help in obtaining NMR data.

**Supplementary Material Available:** Tables of intramolecular distances and angles, least-squares planes, positional parameters, and temperature factor expressions (13 pages); listings of observed and calculated structure factors (85 pages). This material is contained in many libraries on microfiche, immediately follows this article in the microfilm version of the journal, can be ordered from the ACS, and can be downloaded from the Internet; see any current masthead page for ordering information and Internet access instructions.

JA9436207